Toward the characterization of the ATP-binding cassette protein RhaT in *Rhizobium leguminosarum*

by

Derek D. Kim

A Thesis Submitted to the Faculty of Graduate Studies of

The University of Manitoba

In partial fulfillment of the requirements of the degree of

MASTER OF SCIENCE

Department of Microbiology

University of Manitoba

Winnipeg

Copyright © 2019 By Derek D. Kim

Abstract

ATP-binding cassette (ABC) transporters are found throughout all domains of life. Sugar importers are often categorized under the Carbohydrate Uptake Transporter (CUT) system. This classification system is based on the structure of the ABC, in which CUT1 ABCs are comprised of a dimer of two peptides and CUT2s are believed to consist of a single protein. A novel ABC transporter interaction was previously discovered in *Rhizobium leguminosarum*. The transport activity of the L-rhamnose importer was found to be dependent on an interaction between the sugar kinase (RhaK) and a CUT2 ABC protein (RhaT). In this work, a partial *rhaT* deletion mutant was found to retain the ability to grow on rhamnose as a sole carbon source, despite missing a substantial portion of its internal region. Through *in silico* approaches, this partial deletion was characterized and two *rhaT* truncation mutants were designed to truncate a CUT2 ABC to resemble a CUT1. Although transport rates were greatly reduced, these truncation mutants were able to preserve growth, supporting the feasibility of converting a CUT2 transporter to CUT1. In addition, *rhaT* deletions were unable to be complemented by *rhaT* as an independent gene *in trans*. Complementation of this gene using a multigene transcript was found as a potential workaround to complement this membrane protein. These findings will likely help steer towards characterizing RhaT in the context of its interaction with the kinase RhaK.

Acknowledgments

First and foremost, I would like to thank my supervisor Dr. Ivan Oresnik. Under his care, I learned lifelong lessons with every misstep I made. The warmth (though the lab itself is too cold) and cooperative atmosphere of our research group is a testament to his great mentorship. Deciding to join this lab has been one of the best decisions I have made in my life.

I have also been blessed with such a supportive advisory committee. They have always been so patient and understanding. Special thanks to Dr. Richard Sparling for sacrificing so much of his time to look after my dissertation in such a short notice.

My time here has been unforgettable, thanks to everyone at the Oresnik lab. All those days we sat together and bonded through the good and bad are memories I will cherish forever. You guys are such an amazing group and I am so happy that I got to be a part of it.

Lastly, I want to thank NSERC and UMGF for funding this project. I have learned so much throughout this invaluable experience.

Dedication

I dedicate this thesis to my mother, In Nam, who supported me every step of the way. She gave up so much for my education. Despite being in an unfamiliar place with no support for herself, she always kept up her strong face and looked to my troubles. Thanks, mom. I love you. This is the least I can do to express my gratitude.

Table of Contents

Abstract i
Acknowledgments ii
Dedication iii
Table of Contents iv
List of Tables vi
List of Figures vii
List of Abbreviations viii
Chapter 1: Literature Review 1
1.1 The Underlying Problem 2
1.2 Symbiosis 3
1.2.1 Initiation 3
1.2.2 Organogenesis & Infection 4
1.2.3 Differentiation & Nitrogen Fixation 5
1.3 Competition for Nodule Occupancy 6
1.4 Rhamnose Catabolism 7
1.4.1 Introduction 7
1.4.2 Catabolic Pathway 8
1.4.3 Regulation 9
1.5 ABC Transporters 10
1.5.1 Introduction 10
1.5.2 Nucleotide Binding Domain 13
1.5.3 Transmembrane Domain / Permease 14
1.5.4 Substrate Binding Protein 15
1.5.5 ABC Importer Mechanisms 16
1.5.6 Mechanism-based Classification (Types I, II, III) 17
1.5.7 Mechanistic Differences Between Type I and Type II Transporters 18
1.5.8 NBD-based Classification (CUT 1 & 2) 20
1.6 Project Background: 21
1.7 Thesis Objectives 25
Chapter 2: Materials and Methods 26

2.1 Bacterial Strains and Culture Conditions 27
2.2 DNA Manipulations, Techniques, and Sequencing 31
2.3 Inverse PCR for the Construction of Rlt278 and Rlt279 31
2.4 Gibson Assembly Cloning 32
2.5 Transport Assays 32
2.6 Growth Curves 33
2.7 Bioinformatic Analysis 34
Chapter 3: Results 35
3.1 Investigation of RhaK-RhaT interaction using *rhaT* deletion mutants 36
3.2 RhaT is unable to be complemented on a plasmid. 38
3.3 Slow growing phenotype of the truncated RhaT in Rlt278. 40
3.4 Analysis of the truncated *rhaT* in Rlt278 43
3.5 Designing a CUT1 rhamnose ABC protein 45
3.6 Determination of a truncation site 53
3.7 The truncated RhaT can utilize rhamnose as a sole carbon source. 58
3.8 Accumulation of rhamnose in *rhaT* truncation mutants 60
3.9 Complementation of *rhaT* as a polygenic transcript 63
Chapter 4: Discussion 65
Chapter 5: Conclusions 74
Literature Cited 76

List of Tables

Table 1. List of bacterial strains used in this work. 28
Table 2. List of primers used in this work. 30
Table 3. Complementation of *rhaT* deletion strains. 39
Table 4. Generation time of rhamnose locus mutants. 42
Table 5. Generation time of *rhaT* CUT1 conversion mutants. 59
Table 6. Accumulation of rhamnose in *rhaT* deletion mutants over 1 hour. 62
Table 7. *rhaT* complementation in rhamnose deletion mutants using rhamnose locus cosmids carrying transposon insertions. 64

List of Figures

Figure 1. A schematic diagram of an ABC importer. 12
Figure 2. Rhamnose catabolism locus in *Rhizobium leguminosarum* bv. *trifolii*. 23
Figure 3. Construction of the truncated *rhaT* (Rlt278) using inverse PCR. 37
Figure 4. Growth rates of *rhaT* deletion mutants. 41
Figure 5. Amino acid sequence of the truncated RhaT in Rlt278. 44
Figure 6. Multiple sequence alignment of CUT1 ABC proteins and truncated RhaT. 51
Figure 7. Motif layouts of CUT1 ABCs and the truncated RhaT. 52
Figure 8. First truncation site of the CUT1-like *rhaT* construct. 54
Figure 9. Second truncation site of the CUT1-like *rhaT* construct. 56
Figure 10. Predicted structure of truncated RhaT, FrcA, and MalK. 57
Figure 11. Accumulation of [^{3}H] L-rhamnose in *rhaT* truncation mutants over 1 minute.. 61
Figure 12. Uptake curve of *rhaT* truncation mutants. 69

List of Abbreviations

ABC = ATP-binding cassette

NBD = Nucleotide Binding Domain (of ABC transporters)

TMD = Transmembrane Domain (of ABC transporters)

TMS = Transmembrane Segment (of TMD)

SBP = Substrate Binding Protein (of ABC transporters)

ATP = Adenosine triphosphate

ATPase = Adenosine triphosphatase

Mg^{2+} = Magnesium ion

Kd = Dissociation constant

spp. = Species (plural)

CUT = Carbohydrate Uptake Transporter

AA = Amino Acid

^{3}H = Tritium (a radioactive isotope of hydrogen)

NEB = New England Biolabs

bp = Base pairs (of DNA)

TY = Tryptone Yeast

VMM = Vincent's Minimal Media

Glc = Glucose

Rha = Rhamnose

Sm = Streptomycin

Tc = Tetracycline

Tn = Transposon

Cm = Chloramphenicol

Gm = Gentamicin

Amp = Ampicillin

Nm = Neomycin

Km = Kanamycin

NG = No Growth

CDD = NCBI Conserved Domain Database

BLAST = Basic Local Alignment Search Tool

PRALINE = Profile Alignment

BLOSUM = Block Substitution Matrix

PCR = Polymerase Chain Reaction

PHYRE = Protein Homology/Analogy Recognition Engine

Chapter 1:

Literature Review

1.1 The Underlying Problem

The discovery of ammonia synthesis by Fritz Haber and the subsequent industrial scaling of the process by Carl Bosch has revolutionized agriculture and changed the course of human history (Barona *et al.* 2018). Historically, nitrogen has been a limiting nutrient in growing crops. In all biological lifeforms on Earth, nitrogen plays an essential role in the biosynthesis of nucleic acids, amino acids, and other vital processes. However, a significant proportion of the element is inaccessible for most organisms due to it occurring in gaseous dinitrogen state. The abundance of affordable ammonia for agricultural deployment has rendered the issue a relic of a bygone era, bringing down the price of food globally and allowing traditionally nutrient-poor soils to support larger populations (Barona *et al.* 2018). As a result of this innovation, the global population has increased exponentially within the past century.

The issues faced in modern times are on the opposite side of that spectrum. It is estimated that only 50% of nitrogen inputs in the soil are utilized by the plant and the remainder are washed away by irrigation or by precipitation (Savci 2012). Excessive amounts of nitrogen runoff are carried into aquatic systems, contributing to increasingly common issues such as algae blooms. In addition, the Haber-Bosch process itself has high energy demands, which are traditionally fulfilled by fossil fuel combustion. Today, the nitrogen synthesis for agriculture is twice the pre-industrial natural rate generated in terrestrial ecosystems (Erisman *et al.* 2015). With over half of the world's crops dependent on nitrogen fertilizers (Smil 2011), humanity is overproducing its way to environmental calamity. Production of synthetic ammonia is said to be responsible for 2% of the world's total energy expenditure and 1.6% of global CO_2 emissions (Liu 2014). Limiting the production of synthetic fertilizers and transitioning to sustainable

technologies will be essential in mitigating the increase in global temperature due to heat entrapment by greenhouse gases.

1.2 Symbiosis

In nature, there are several ways that plants have adapted to overcome the limitation of the finite concentrations of usable nitrogen. One of these strategies is mutualistic interaction with diazotrophic bacteria. Legumes, which are producers of plant-based protein, are known to form symbiotic interactions with a group of diazotrophs termed rhizobia. Rhizobia are Gram negative soil bacteria that are capable of both saprophytic and endophytic lifestyles. This group of organisms attracted great interest from both academia and industry due to its ability to fix atmospheric nitrogen into organic forms of nitrogen to result in a net beneficial outcome for its host once in its endosymbiotic state.

1.2.1 Initiation

This symbiotic association is initiated through the recognition of compatible host flavonoid signalling molecules by saprophytic rhizobia. The recognition of specific flavonoids triggers the transcriptional activation of *nod*, *nol*, and *noe* genes, resulting in the production of bacterial signalling molecules called Nod factors. These molecules are characterized as lipochitooligosaccharides with 4 or 5 N-acetylglucosamine residues with their non-reducing terminal residues positioned at the second carbon with an attached acyl chain, with sugar substituents decorating the terminal sugar (Bisseling 2002; Oldroyd 2013). The structure of the acyl chains and side residues vary based on the rhizobial species, and these structural distinctions

ultimately contribute to host specificity. Mutations in Nod factor biosynthesis have shown that rhizobia cannot colonize its host in the absence of Nod factors (Downie and Walker 1999). Other signalling molecules found to play a role in nodulation include exopolysaccharides, lipopolysaccharides, cyclic glucans, and capsular polysaccharides (Via *et al.* 2016).

These molecules are recognized by surface receptors of the host plant, such as the LysM-family receptor kinases responsible for the initiation of nodulation through binding Nod factors and exopolysaccharides (Via *et al.* 2016). The structure of these receptor complexes varies depending on the plant. This symbiotic signalling pathway, termed the common Sym pathway, bears similarities to Arbuscular Mycorrhizal symbiosis, which is believed to predate legume-rhizobia symbiosis by hundreds of millions of years (Corradi and Bonfante 2012; Kondorosi *et al.* 2013).

1.2.2 Organogenesis & Infection

The signal exchange between the host and the rhizobia triggers a cascade of physiological changes within the root hair, starting with the rapid oscillations of intracellular calcium levels (Ehrhardt *et al.* 1996). During this process, two important events occur simultaneously to enable symbiosis. The first of the two is nodule organogenesis, which initiates in the inner cortex and pericycle (Timmers *et al.* 1999). Nodules are structures situated in the root, which are developed to serve as specialized housing compartments for nitrogen-fixing rhizobial partners. On the surface of the root hair, its tip swells and extends towards the origin of compatible Nod Factors. Eventually, the extending root hair tip reaches the source of Nod Factors and the bacteria are able to attach to the root hair. This results in the root hair curling on itself forming a tightly

curled branch, trapping the rhizobia inside a compartment termed “Shepherd’s crook” or “Curled-colonized root hair” (Esseling *et al.* 2003). Once the bacterium is inside this compartment, it must eventually reach the nodule being developed in the cortex. In order for this to occur, the plant forms invaginations along its root hair down to the cortex. Rhizobial cells also produce cellulases to progress through these structures. It is within these “infection threads” that rhizobial cells divide to reach the developing nodule (Robledo *et al.* 2008). The formation of infection threads is believed to be dependent on the threshold of Nod Factors being produced as the rhizobial population inside the compartment increases. Plant hormones like cytokinin are required for proper targeting of root cortical cells during infection thread formation. Mutations of cytokinin receptors cause the infection thread formation to become untargeted (Miwa *et al.* 2006).

1.2.3 Differentiation & Nitrogen Fixation

Rhizobial cells that have proliferated to the cortical cells are endocytosed. They become enclosed in an unwalled infection thread-derived membrane called the symbiosome (Jones *et al.* 2007). In indeterminate nodules such as the hosts of *Rhizobium leguminosarum,* the rhizobial cell and its symbiosome replicate synchronously until the rhizobia eventually differentiate into bacteroids. These bacteroids are terminally differentiated and thus, cannot proliferate outside of the nodule. For *Sinorhizobium meliloti,* another rhizobial species that forms indeterminate nodules, only 0.8% of bacteroids gave rise to colonies on agar plates (Mergaert *et al.* 2006). One of the key characteristics of bacteroid differentiation is the endoreplication of its genetic material and the induction of its nitrogen fixation genes while repressing genes involved in growth (Poole

et al. 2018). In essence, the differentiation causes the rhizobial cell to become an optimized nitrogen-fixing organelle-like state.

The nitrogenase enzyme produced by the bacteroid is capable of reducing N_2 to ammonia in a low-oxygen environment. In order to maintain this microaerobic state, the cell employs a haem-containing protein known as leghemoglobin to sequester oxygen. This regulation of oxygen levels controls the expression of nitrogen fixation genes and nitrogenase activity (King *et al.* 1988).

1.3 Competition for Nodule Occupancy

Symbiotic rhizobia have become strong candidates for agricultural biofertilizers as they can fulfill the nitrogen needs of its host plant while minimizing the excess nitrogen runoff or the energy demands for synthesizing ammonia fertilizers. Before rhizobial inoculants can ever fully replace synthesized nitrogen fertilizers in commercial agriculture, there is a major obstacle which must be dealt with. The Earth Microbiome project revealed that alpha-proteobacteria, which includes members of the Rhizobiaceae, are the most abundant class of bacteria in soils around the globe (Delgado-Baquerizo *et al.* 2018). Although rhizobia are common in the soil, their abundance works against the interest of rhizobial inoculants. This problem begins with the fact that the ability to nodulate host plants is independent from its ability to symbiotically fix nitrogen. When non-symbiotic rhizobia nodulate the host plant, the host cannot interact with symbiotic rhizobia. Thus, the presence of non-symbiotic rhizobia in the field has been shown to impede the efficacy of symbiotic inoculants (Dowling and Broughton 1986). There have been

several temporary strategies developed to alleviate this problem, but the underlying issue persists (Triplett and Sadowsky 1992).

To combat the rhizobial competition problem, researchers have scoured through the genomes of rhizobia for genetic determinants in the hope of giving inoculants a competitive edge when deployed in the field. As there has been evidence of metabolic potential being correlated with increased competitiveness, carbon metabolism has become a subject of interest in rhizobial competition research (Geddes and Oresnik 2014). The ability to utilize rhamnose has been identified as one such determinant in *Rhizobium leguminosarum* and *Sinorhizobium meliloti*. Mutants unable to grow on rhamnose as a sole carbon source were found to be severely impaired in competition for nodule occupancy compared to the wildtype (Oresnik *et al.* 1998).

1.4 Rhamnose Catabolism

1.4.1 Introduction

L-rhamnose is a naturally occurring methyl pentose that is primarily found in rhamnogalacturonan, a component of the plant cell wall (McNeil *et al.* 1984). It is also a major constituent of bacterial cell walls in both Gram positive and negative bacteria. In Gram positive bacteria such as *Streptococcus* spp., L-rhamnose is a major part of the cell wall and has been shown to play a critical role in virulence (Mistou *et al.* 2016). It is a constituent of the O-antigen in the lipopolysaccharide (LPS) cell walls of several Gram negative bacteria (Giraud and Naismith 2000). As a common substrate in plant-associated environments, catabolic machinery

for this substrate can be found in a diverse range of organisms. Since rhamnose metabolism has never been identified in higher-order eukaryotes, it has captured the interest of pharmaceutical researchers as a potential drug target for combating microbial diseases (Giraud and Naismith 2000). The breakdown of L-rhamnose has been of great interest in both academia and industry due to its potential for the enzymatic production of a wide range of rare sugars such as D-allose, D-gulose, L-lyxose, L-mannose, L-talose, and L-galactose (Xu *et al.* 2016). Outside of academic use, these rare sugars are highly sought after for their applications in food enhancement and pharmaceuticals.

1.4.2 Catabolic Pathway

The catabolic pathway for L-rhamnose has been well-characterized in *Enterobacteriaceae*. Since its extensive characterization, it has been used as a model to understand similar pathways in other organisms (Rodionova *et al.* 2013). The Kyoto Encyclopedia of Genes and Genomes (KEGG) lists two prominent pathways for L-rhamnose catabolism (Kanehisa and Goto 2000). In fungi and some other eukaryotes, L-rhamnose is converted to L-rhamno-1,4-lactone through a dehydrogenase reaction, and proceeds to be broken down into L-lactaldehyde or 2,4-diketo-3-deoxy-L-fuconate, both of which feeds into pyruvate metabolism. This pathway has also been found in *Sphingomonas* spp. and *Azotobacter vinelandii* (Watanabe *et al.* 2008; Watanabe and Makino 2009). In contrast, most prokaryotes are stated to isomerize L-rhamnose into L-rhamnulose, which is then phosphorylated by a kinase to L-rhamnulose-1-phosphate, which is further catabolized into L-lactaldehyde and dihydroxyacetone phosphate / glycerone phosphate. While both pathways contribute to pyruvate metabolism, the pathway found in prokaryotes is distinct in that it also directly feeds into glycolysis.

The classic pathway based on the enterobacteria model involves three main reactions (Badia *et al.* 1989). The first reaction that occurs following transport, is the isomerization of L-rhamnose into L-rhamnulose. After that, it is phosphorylated into L-rhamnulose by a rhamnulose kinase. The third reaction involves an aldolase, resulting in the breakdown of rhamnulose-1-phosphate into L-lactaldehyde and dihydroxyacetone phosphate, the latter of which feeds directly into central carbon metabolism (Schwartz *et al.* 1974). The fate of the L-lactaldehyde varies system to system, either being converted to L-1,2-propanediol by a reductase such as in *Salmonella typhimurium*, or to L-lactate by a dehydrogenase in some genera including *Erwinia* and *Mannheimia* spp (Rodionova *et al.* 2013).

1.4.3 Regulation

The regulation of the rhamnose catabolism locus features extensive diversity, with at least seven non-orthologous transcription factors that have been found to control L-rhamnose catabolism in bacteria (Rodionova *et al.* 2013). This is due to the sheer breadth in rhamnose operon structures across prokaryotic lineages. These regulators fall into three different superfamilies: AraC, LacI, and DeoR. In Enterobacteriales, the positive AraC-family regulators are the most predominant (Rodionova *et al.* 2013). AraC-family regulators also are found in Bacteroidales, but they are non-orthologous to the AraC transcription factors in Enterobacteriales (Patel *et al.* 2008). LacI regulators are most represented in Actinomycetales (Rodionova *et al.* 2013). DeoR family negative regulators are found throughout the L-rhamnose loci of alpha-proteobacteria and Chloroflexi (Rodionova *et al.* 2013). In *Rhizobium leguminosarum* and

Sinorhizobium meliloti, the L-rhamnose catabolism loci are in a single regulon under a DeoR-family RhaR (Richardson *et al.* 2004).

1.5 ABC Transporters

1.5.1 Introduction

ATP-binding cassette (ABC) transporters are ubiquitous in any biological lifeform on Earth. Biological processes require molecules which often require active transport to traverse across the cellular membrane. The ABC transporter family is one of the largest transporter families known (Zheng *et al.* 2013). These primary transporters use energy from the hydrolysis of ATP to undergo conformational changes that move the substrate across the membrane. It is estimated that 10-60% of the total ATP budget of bacteria and humans is expended by ABC transporters (Rees *et al.* 2009).

Every ABC transporter characterized to date is unidirectional. Each transporter can either export or import substrates but cannot perform both. Despite being labelled as one family, there is a tremendous amount of diversity among its members. This is attributed to ABC transporters being found throughout phylogenetically distant systems as they fulfill a basic cellular need of substrate translocation. These transporters were first discovered in *Escherichia coli* and *Salmonella typhimurium* as periplasmic protein-dependent transporters and later, similar transporters were discovered in Gram positive bacteria, archaea, and eukaryotes (Ames 1986; Hyde *et al.* 1990; Eitinger *et al.* 2011). ABC transporters can be divided into two functional categories: importers and exporters. While exporters can be seen throughout all three domains of

life, importers are historically described to be exclusive to prokaryotes. The discovery of some plant ABC importers identified in *Arabidopsis thaliana* and *Coptis japonica* has challenged the canonical view of ABC importers being limited to prokaryotes (Shitan *et al.* 2003; Santelia *et al.* 2005; Terasaka *et al.* 2005). ABC exporters such as the human P-glycoproteins (Pgp) are currently a hot topic in research due to their involvement in multidrug resistance and pathogenicity. Importers play a role in supplying essential nutrients to be consumed in metabolic processes. In the cell, these importers play a key role in a vast number of functions, including but not limited to: transport of essential cellular nutrients, metals and other growth factors, maintenance of outer membrane lipid distribution, chemotaxis, cell signalling, and virulence (Eitinger *et al.* 2011).

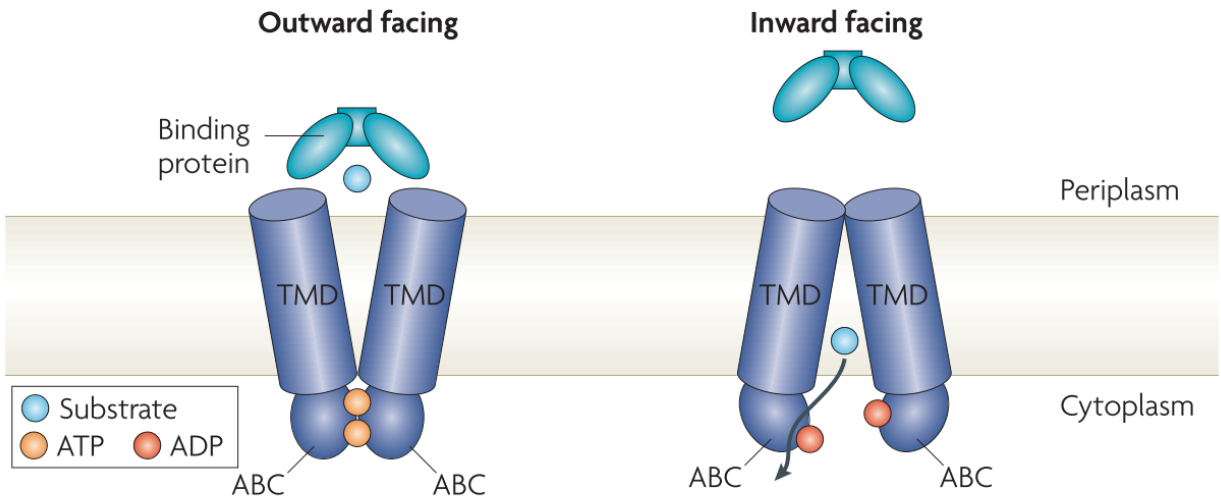

Figure 1. A schematic diagram of an ABC importer.

Reprinted by permission from Copyright Clearance Center RightsLink®: Springer Nature. Nature Reviews Molecular Cell Biology. ABC transporters: the power to change, Douglas C. Rees *et al*., © March 1, 2009.

1.5.2 Nucleotide Binding Domain

An ABC transporter is typically comprised of two core components: two transmembrane domains (TMD) and two nucleotide-binding domains (NBD). The NBDs are responsible for the ATPase activity required for the hydrolysis of ATP, enabling active transport. Traditionally described as a dimer, NBDs form a tight interface between each other, and it is the distance between the NBDs that dictate the conformational state of the transporter (Locher 2016). This dimeric structure can either exist as two separate proteins or as a single peptide, the latter of which can be found in some prokaryotic ABC importers (Eitinger *et al.* 2011). The NBD is highly conserved. It is a L-shaped structure organized into two "arms" (Hopfner 2016). The first (Arm I) is described as the catalytic domain and contains the P-loop / Walker A, Walker B, and the H-loop / Switch region (Schmitt and Tampe 2002). ATP is bound at the alpha- and beta-phosphates by the P-loop / Walker A motif and at the adenine by the A-loop, constituting the catalytic domain (Walker *et al.* 1982). The Walker B motif contains residues which bind the Mg^{2+} cofactor, participate in the ATP hydrolysis reaction, and interacts with the Walker A motif via its catalytic glutamate residue (Walker *et al.* 1982). The H-loop located in a region termed "Switch II" is responsible for stabilizing the transition-state (Zhou *et al.* 2013). It accomplishes this by acting as a general acid and base, facilitating the transfer of protons during the reaction. The structure of this arm is described to be a homologue of RecA and F_1-ATPase (Story and Steitz 1992; Abrahams *et al.* 1994).

Arm II, also called the signalling domain, is a region which is comprised solely of α-helices and has no structural homologues outside of the ABC superfamily (Schmitt and Tampe

2002). This region contains the ABC signature motif / C-loop and Q-loop. The ABC signature motif, defined by its conserved LSGGQ sequence, is crucial for the proper orientation of the NBD and its ability to impose conformational changes through interacting with its dimer pair. The p-loop must always face the signature motif (LSGGQ) in the alpha-helical domain of its adjacent dimer pair, which works to localize and orient ATP during its hydrolysis (Rees *et al.* 2009; Locher 2016). This signature motif can be used to identify sequences of ATPases belonging to the ATP transporter family. The Q-loop acts as the contact point for the interface between the NBD and Transmembrane Domain (TMD). The region where the Q-loop is located has relatively high variance, which is hypothesized to provide a distinct signature "barcode" to increase selectivity to its intended TMD partner (Schmitt *et al.* 2003).

1.5.3 Transmembrane Domain / Permease

The transporter permeases / transmembrane domains are highly variable proteins that are involved in substrate specificity and in the formation of the physical passageway through the membrane. Similar to NBDs, TMDs work as a dimer pair. For each given substrate, the TMDs of the corresponding ABC importers will have a distinct set of transmembrane helices, ranging from anywhere from 5 to 10 and rarely possess sequence homologies with one another (Schneider *et al.* 2012). Some TMDs, such as MalF in the maltose transporter in *E. coli*, possess a substrate-binding site to stabilize and increase affinity to its substrate (Oldham *et al.* 2007). A region called the coupling helices forms the contact interface between the Q-loop (NBD) and the coupling helices (TMD) (Blüschke *et al.* 2007). This conserved region defined by its EAA motif (EAA-X3-G-X9-I-X-LP), an identifying marker of ABC transporter TMDs (Saurin *et al.* 1994).

The conformational changes resulting from ATP hydrolysis is thought to be caused by noncovalent interactions in this interface (Eitinger *et al.* 2011).

1.5.4 Substrate Binding Protein

Prokaryotic ABC importers, with the exception of Energy Coupling Factor (ECF)-family importers, possess a protein called the substrate-binding protein (SBP). These proteins are characterized by a high affinity to their substrates, ranging from 0.01 to 1 μM in Kd values and are essential in capturing the substrate and presenting it to the transporter complex (Eitinger *et al.* 2011). In Gram negative bacteria, the SBPs diffuse freely in the periplasmic space (van der Heide and Poolman 2002). In Gram positives, some genera of cyanobacteria, and some archaea, SBPs are lipoproteins anchored to the outer surface of the cellular membrane by a N-terminal lipid moiety, and between 2 to 6 SBPs are associated with each transporter complex (Sutcliffe and Russell 1995). There have also been characterized SBPs that are in permanent association to TMDs (Biemans-Oldehinkel *et al.* 2006; Daus *et al.* 2007).

SBPs are made up of two symmetrical domains (Quiocho and Ledvina 1996). These domains possess an alpha / beta fold and are connected by a hinge region (Davidson *et al.* 2008). The substrate-binding site lies within a cleft between the two domains. In this site, the specificity of the substrate is determined primarily by the differential hydrogen bonding. The mechanism of substrate capture is described as a “Venus trap model”, which begins with the substrate binding causing the inward rotation of the domains. This results in the substrate-binding site being closed off, physically locking the substrate in place (Quiocho and Ledvina 1996).

1.5.5 ABC Importer Mechanisms

The classical mechanism of transport described for ABC importers is the alternating access model. This is based on the mechanism of the maltose importer in *E. coli* and *Salmonella*, the most well-studied importer (Eitinger *et al.* 2011). In this model, the transporter is believed to be in its apo-state when it is ATP-bound and the substrate is absent from the complex (Oldham *et al.* 2008). Binding of the substrate-bound SBP will then result in the ATPase subunits to associate more tightly, opening the channel towards the periplasm. This in turn causes a conformational change in the SBP to release the substrate into the transport channel (Orelle *et al.* 2008). The chemical properties of the substrate were shown to be unimportant in triggering the transport process (Gould and Shilton 2010). According to Eitinger *et al.*, 2011, the steps following this are still speculative. Hydrolysis of one ATP has not been shown to open the transporter inwards and thus is considered insufficient for transport (Daus *et al.* 2007; Grote *et al.* 2008). At most, it is believed to send the substrate further along in the channel. The hydrolysis of the second ATP changes the conformation to the inward facing state towards the cytoplasm. Binding of ATP is required to return the complex to its resting state. Ultimately, the model requires the hydrolysis of 2 ATP molecules for the transport of one substrate molecule.

However, the discovery of transporters with single fused ATPases brings this model into question. Some of these single peptide ATPases (categorized as members of the CUT 2 family) have been characterized as possessing only a single functional ATP-binding site, as the P-loop in the second NBD of CUT2 family ATPases possess a substitution in its conserved lysine residue. This substitution from lysine to arginine has been shown to abolish ATP hydrolysis activity

(Schneider and Hunke 1998). There was also a class of ABC exporters with a nonfunctional NBD that was found to perform successful transport with only a single functional ATP-binding site (Ernst *et al.* 2008). This suggests that there is not a single unifying mechanistic model for all ABC transporters.

1.5.6 Mechanism-based Classification (Types I, II, III)

The most prominent classification system for ABC transporters is based on its mechanism of transport. This classification (I, II, III) moves beyond the "one-size-fits-all" traditional alternating access model of ABC transporters. There are currently three types categorized by this system. Type I importers are typically known to transport metabolites while type II importers transport trace elements and growth factors such as vitamins and iron complexes. Type II importers have a much higher affinity to their substrate than Type I importers. This reflects the relative abundance of the substrates for Type I compared to that of substrates for Type II importers (Locher 2016; Lewinson and Livnat-Levanon 2017). Substrates of Type I importers are often abundant in its environment or can be metabolically converted from a different substrate. In contrast, substrates of Type II ABC importers are commonly essential growth factors that are available only in trace quantities. The disparity in abundance places an evolutionary pressure to ensure transport of the relatively rare substrates even at the cost of constant energy expenditure, while transporting the abundant substrates only when required.

Type III importers are uptake transporters which lack solute-binding receptors/proteins (SBPs) and are also known as the Energy Coupling Factor (ECF) superfamily, which transport

vitamins, metal ions, or amino acids (Locher 2016). This group is characterized as having one conserved TMD, two NBDs, and an additional integral membrane protein (S-component) that functionally substitutes the role of SBP in substrate capture (Eitinger *et al.* 2011).

1.5.7 Mechanistic Differences Between Type I and Type II Transporters

In a Type I transporter, the N and C terminal lobes of its associated SBP are connected by flexible loops. When it binds the substrate, it acts in accordance to the Venus flytrap model and the conformation of the holo state is distinct from the apo state. Type I importers only initiate NBD constriction with the docking of the holo SBP (Davidson *et al.* 1992; Patzlaff *et al.* 2003). In its resting state, the TMDs face towards the cytoplasm and the NBDs are separated with ATPs bound. Initial contact with SBP reorient the TMDs outward, allowing SBP to dock. SBP interaction with transporter is described as transient.

In contrast, the N and C terminal lobes of Type II SBPs are connected by a rigid alpha helix, which results in a similar state for both holo and apo states. As a result, they are so similar that the transporter will be insensitive to the holo SBP and respond in the same way as if an unbound SBP was to dock to the TMD (Borths *et al.* 2005). A defining characteristic of Type II is that there is a basal level of ATP hydrolysis activity present even in the absence of the SBP and its substrate (Lewinson and Livnat-Levanon 2017). In addition, SBPs in Type II systems form stable complexes with the transporter. The SBP docking site is always present in the TMDs and there are very little structural changes in the TMD throughout the course of the transport process.

In both Types, loops from the TMD protrude into the SBP to disturb the binding pocket to release the substrate into the channel (Hvorup *et al.* 2007; Oldham *et al.* 2013). In Type I, the state in which the substrate resides within the channel is a high-energy intermediate state that is quickly resolved by ATP hydrolysis and the ensuing conformational changes. In Type II, the channel possesses several residues that act similarly to gates in ion channels. As the substrate makes its way through the TMD, there is local movement of key residues that close off and "squeeze" the substrate through. It has been described as a peristalsis-like process (Korkhov *et al.* 2014). There has been empirical evidence to support a spontaneous release of the substrate from the channel but that finding is currently a point of contention in the subject area (Lewinson and Livnat-Levanon 2017).

Following the release of the substrate into the cytoplasm, the transporter resets for the next transport cycle. In Type I, the hydrolysis of ATP triggers the release of the SBP and shortly after, ADP dissociates from the NBD. This frees up the ATP-binding site to capture a free cytoplasmic ATP to return the complex to its resting state. On the other hand, the mechanism of transport reset in Type II importers remains an active research focus. The release of the substrate has shown to yield the lowest energy state of the transporter (Lewinson *et al.* 2010). Based on the stoichiometry of ATP to vitamin B_{12} transport, it is believed that several rounds of ATP hydrolysis may be required for the dissociation of the SBP from the complex (Tal *et al.* 2013). Unlike in Type I transporters where TMDs and NBDs reciprocate each other's movement, Type II TMDs and NBDs were found to be conformationally decoupled (Vigonsky *et al.* 2013; Joseph *et al.* 2014). In these studies, the TMDs did not undergo any conformational changes in response to NBD conformational changes due to ATP hydrolysis in the absence of the substrate. This finding suggested that an ATP hydrolysis cycle in the absence of the substrate can trigger

movement in the NBD without affecting the TMDs. While this futile ATPase activity appears at first glance to have an adverse effect on the transporter, the opposite has been observed. Empirical evidence showed a longer preservation of stability in ATPases that were subjected to constant ATP hydrolysis in a substrate-free environment as well as higher transport rates after reconstitution into liposomes (Livnat-Levanon *et al.* 2016). This corroborates the hypothesis in which several rounds of ATP hydrolysis are required for complete transport (Lewinson and Livnat-Levanon 2017).

1.5.8 NBD-based Classification (CUT 1 & 2)

Carbohydrate importers can be categorized further in a different school of classification. First described by M. Saier, this system groups importers into Carbohydrate Uptake Transporter 1 (CUT1) or CUT2 (Saier 2000). Transporters are classified based on their structure, notably the cytoplasmic Nucleotide Binding Domain (NBD). CUT1 is believed to have a dimer of 2 NBDs of 300 amino acids per peptide. An example of CUT1 is the *E. coli* maltose transporter MalFGK. CUT2 is thought to have a single NBD of 500 amino acids with a single active site, possibly due to a fusion of the two NBDs halves of the dimer (Schneider 2001). This is supported by the finding of a region in the CUT2 NBD that appears to be a vestige of an ATP binding site (Schneider 2001). In this region, there is a substitution of a conserved lysine residue in the P-loop to an arginine. Substitution of this conserved lysine has been shown to abolish ATP hydrolysis activity (Schneider and Hunke 1998). This categorization is a part of a larger collection of ABC transporters in the Transporter Classification (TC) system managed by the Saier group (Saier *et al*. 2016). According to the database, there are also some differences in the number of transmembrane segments (TMS) of the TMDs observed between characterized CUT1

and CUT2 systems. From a collection of 35 entries of characterized CUT1 transporters in the database, the number of TMS ranges from 6 to 8 with a mean of 6.6 ± 1.1 and a median of 6. For CUT2, there are 16 entries with TMS ranging between 7 to 12, averaging 9.4 +- 1.1 with a median of 10 (Zheng *et al.* 2013).

Since the last review of the CUT classification system, there has been a lack of development in its differentiation criteria. Although this classification system has not been explored with the same degree of rigour as the mechanism-based system, the CUT system continues to be used regularly in publications characterizing carbohydrate importers (Pinweha *et al.* 2018; Wagner *et al.* 2018; Huang *et al.* 2019; Ravindranathan *et al.* 2019).

1.6 Project Background:

The rhamnose transporter in *Rhizobium leguminosarum* bv. *trifolii* initially became a research interest when transposon mutants incapable of growing on defined media supplemented with rhamnose as a sole carbon source were found to be substantially impaired in their ability to compete for nodule occupancy in comparison to their wild-type counterpart Rlt100 (Oresnik *et al.* 1998). In order to better understand the reasons why these mutants are uncompetitive, the rhamnose catabolism locus in *R. leguminosarum* was characterized (Richardson *et al.* 2004). Using a series of transposon mutants generated in the cosmid pW3C1, which was found to complement rhamnose and sorbitol catabolism in the plasmid-cured strain Rlt101, the genes in the locus were identified. The rhamnose locus was found to consist of two transcripts. The first of the transcripts was found to encode for an aldolase (*rhaD*) followed by an isomerase (*rhaI*)

(Figure 2). The other transcript is preceded by a DeoR-family regulator (*rhaR*). This family is named after the *deo* operon in *E. coli* (Mortensen *et al.* 1989). The majority of DeoR family regulators act as repressors, including the glycerol catabolism repressor GlpR in *E. coli* and *Rhizobium leguminosarum* bv. *viciae* (Schweizer *et al.* 1985; Ding *et al.* 2012). In accordance with this trend, *rhaR* was also characterized to be a repressor of the rhamnose operon. Following *rhaR*, genes encoding an ABC transporter were identified. This transporter is encoded as follows: SBP (*rhaS*), ATPase (*rhaT*), followed by heterodimeric TMD / permeases (*rhaP* and *rhaQ*) (Figure 2). Downstream of the transporter genes, there is a mutarotase (*rhaU*) and then a sugar kinase (*rhaK*) (Figure 2).

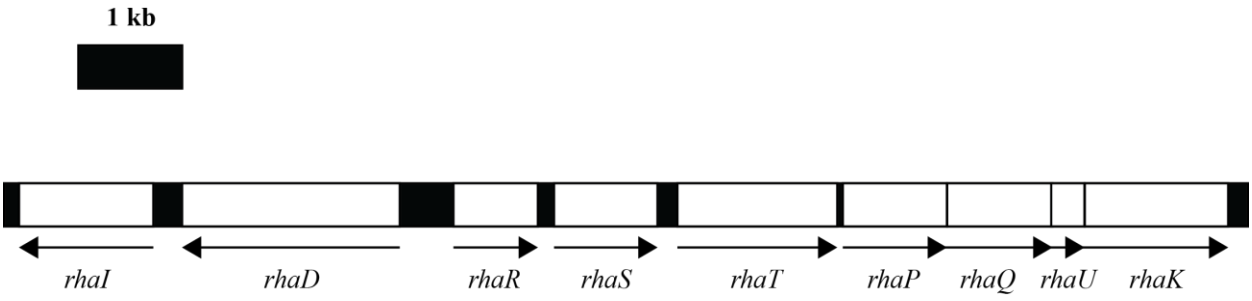

Figure 2. Rhamnose catabolism locus in *Rhizobium leguminosarum* bv. *trifolii*.

Genes within this locus are represented to scale. Open bars with arrows correspond to the open reading frame of the gene listed underneath the bar. Closed bars represent non-coding regions. Sequence data was collected from GenBank (NCBI Accession Number: NG_035912.1) (Richardson *et al*. 2004).

Investigation of the sugar kinase RhaK revealed its enigmatic nature. The canonical rhamnose catabolism pathway using the *E. coli* model initiates with the isomerization of rhamnose into rhamnulose. The kinase phosphorylates rhamnulose into rhamnulose-1-phosphate, which is then cleaved into dihydroxyacetone phosphate and lactaldehyde (Rodionova *et al.* 2013). However, RhaK was found to have rhamnose kinase activity, which at the time suggested an alternate catabolism pathway involving the phosphorylation of rhamnose preceding its isomerization. In constrast, RhaK in *Sinorhizobium meliloti* does not appear to possess any rhamnose kinase activity (unpublished data). In light of this finding, it was speculated that the phosphorylation of rhamnose in *R. leguminosarum* may instead serve a regulatory purpose.

In addition to the rhamnose kinase activity of RhaK, it was also found to be essential to perform transport. Several strains with a transposon insertion in *rhaK* showed a complete abolishment of rhamnose transport (Richardson and Oresnik 2007). These mutations were confirmed to have no adverse effects on either transcription or translation of the transporter and the resulting phenotype was shown to be complemented by *rhaK in trans*. The involvement of RhaK was shown to involve the catabolic sites, as mutations in any of the key ATP-binding residues resulted in the disruption of transport. While the transport dependency on a functional kinase structure in RhaK could not be decoupled, two alleles were discovered to affect transport without being involved in the phosphorylation activity (Rivers and Oresnik 2013). Identification of these two alleles, *rhaK72* and *rhaK73*, revealed that they are located near the N- (*rhaK73*) and C- (*rhaK72*) termini of the peptide. According to predicted structural models of RhaK, these alleles are located on the surface of each of the “lobes” of the clamp-like kinase, oriented along the same face. This finding was followed up by a two-hybrid interaction study, which showed

protein-protein interaction between fragments containing wild-type versions of these two alleles and the cytoplasmic N-terminal fragment of the ATPase (RhaT) (Rivers and Oresnik 2015).

Currently, there are no other characterized ABC importers that interact with their sugar kinase to enable transport described in the literature. The discovery of this putative novel interaction propelled the investigation into the mechanism of a new ABC importer mechanism. These studies were replicated in *Sinorhizobium meliloti*, a well-characterized symbiotic diazotroph and another member of the Rhizobiaceae (unpublished data). These results shown in *S. meliloti* corroborated the existence of a novel type of ABC importer in the Rhizobiaceae.

1.7 Thesis Objectives

This thesis aims to continue the investigation of the rhamnose transporter and the novel interaction between RhaK and RhaT. Previous evidence corroborates the likelihood that the RhaSTPQ system is the only rhamnose importer in *Rhizobium leguminosarum* as well as *Sinorhizobium meliloti*, which make them promising candidates as model systems for the investigation of a novel importer mechanism. In this work, a partial deletion mutant of *rhaT* was constructed for complementation. However, the complementation was unsuccessful, and the partial deletion mutant retained growth on rhamnose. The main objective of this work was to analyze the truncated RhaT, and to determine the mechanism through which it is maintaining its ABC function. This work also sought to find an alternative strategy for plasmid complementation of *rhaT*.

Chapter 2:

Materials and Methods

2.1 Bacterial Strains and Culture Conditions

Bacterial strains and plasmids used in this work are listed in Table strains. *Escherichia coli* and *Sinorhizobium meliloti* strains were grown at 37°C in Lysogeny broth (LB) as complex medium (Sambrook and Russell 2001). *Rhizobium leguminosarum* strains were grown at 28°C in Tryptone Yeast (TY) as complex medium and Vincent's Minimal Medium (VMM) as defined medium (Vincent 1970; Beringer 1974). On defined media, carbon substrates were filter sterilized and added at a final concentration of 15 mM. When required, antibiotics were added to solid growth media at the following concentrations: tetracycline at 5 µg ml^{-1}, streptomycin at 200 µg ml^{-1}, ampicillin at 100 µg ml^{-1}, chloramphenicol at 20 µg ml^{-1}, and gentamicin at 20 µg ml^{-1} for *E. coli* strains and 60 µg ml^{-1} for rhizobial strains. In liquid media, antibiotics were added at half the concentration compared to solid media. Bacterial culture titres were measured spectrophotometrically at 600 nm.

Table 1. List of bacterial strains used in this work.

Strain/Plasmid	Relevant Genotypes	Source of reference
***R. leguminosarum* strains**		
Rlt100	W14-2 Sm^r, wild-type	(Baldani *et al.* 1992)
Rlt144	Rlt100 *rhaK50*::Tn*5*-B20	(Richardson *et al.* 2004)
Rlt243	Rlt100 Δ*rhaU*	(Richardson *et al.* 2008)
Rlt278	Rlt100 partial Δ*rhaT* resulting in truncation	This work
Rlt279	Rlt144 partial Δ*rhaT*	This work
Rlt280	Rlt100 complete Δ*rhaT*	This work
Rlt281	Partial Δ*rhaT* NBD2 removed	This work
Rlt282	Truncated *rhaT* (285AA)	This work
Rlt283	Truncated *rhaT* (264AA)	This work
***E. coli* strains**		
DH5α	λ^- φ80d*lacZ*°M15°(*lacZYA-argF)U169 recA1 endA1 hsdR17*(r_k^- m_k^-) *supE44 thi-1 gyrA relA1*	(Hanahan 1983)
MT616	MT607(pRK600)	(Finan *et al.* 1986)
Plasmids		
pBlueScript II SK^+	ColE1 *oriV* Amp^r cloning vector	Stratagene
pJQ200SK	Suicide vector, P15a *ori*, *mob sacB*, Gm^r	(Quandt and Hynes 1993)
pRK7813	RK2 *ori*, pUC9 polylinker, λ *cos* site, Tc^r	(Jones and Gutterson 1987)
pRK600	pRK2013 *npt*::Tn*9* Cm^r Nm^-Km^s	(Finan *et al.* 1986)
pDR197	Wild-type *rhaT* in pRK7813	
pW3C1	pRK7813 cosmid from Rlt100 cosmid bank. Carries rhamnose catabolism locus.	(Oresnik *et al.* 1998)
pW3A	pRK7813 cosmid from Rlt100 cosmid bank. Carries rhamnose catabolism locus.	(Oresnik *et al.* 1998)

pMR73	pW3A *rhaR25*::Tn*5*B20	(Richardson *et al.* 2004)
pW3AR2	pW3A *rhaT2*:Tn*5*B20	(Oresnik *et al.* 1998)
pMR67	pW3A *rhaP19*::Tn*5*	(Richardson *et al.* 2004)
pMR98	pW3A *rhaK50*::Tn*5*B20	(Richardson *et al.* 2004)
pMR110	Wild-type *rhaK* in pRK7813	(Richardson and Oresnik 2007)
pDK7	partial Δ*rhaT* in pJQ200SK	This work

Table 2. List of primers used in this work.

Primer Name	Relevant Sequence (5' → 3')
rhaTDelFlankSF	GAATTCCTGCAGCCCGTTCTCGCTGCCTCCAAG
rhaTDelFlankSR	ATGTTTTTACCCAGATTTCTACCAGTGTCGAAG
rhaTDelFlankPF	AGAAATCTGGGTAAAAACATGGCAAGACTG
rhaTDelFlankPR	CGCTCTAGAACTAGTGCGCGATAGATGGTGAGCG
pdrhaT639TGAF	CTTGATATCGAATTCCTGCAGATGAACGCCGCCTTTCAAC
pdrhaT639TGAR	TGTTTTTACCTCAGATGAAGAGGATCGCC
pdrhaTPFlankF	CTTCATCTGAGGTAAAAACATGGCAAGACTG
pdrhaTPFlankR	TGGAGCTCCACCGCGGTGGCGGCCGCTTTCGTCCAGCCCGTATC
CUT1rhaTFrag_F	TGATATCGAATTCCTGCAGTCCGGAGCCGACGTTTAAG
CUT1rhaTFrag285_R	TGTTTTTACCTCATTCGGTGCGGTGGCT
CUT1rhaTFrag264_R	TGTTTTTACCTCACGGAAAGACGTTCTCG
CUT1rhaPFrag285_F	CCGAATGAGGTAAAAACATGGCAAGACTGATCAGAAAACGC
CUT1rhaPFrag264_F	TTCCGTGAGGTAAAAACATGGCAAGACTGATCAGAAAACGC
CUT1rhaPFrag_R	CCGCTCTAGAACTAGTGGATCCTCATGCTGCGGCCTCCGC

2.2 DNA Manipulations, Techniques, and Sequencing

Standard techniques were used for bacterial plasmid isolation, agarose gel electrophoresis, restriction enzyme digestion, DNA ligation, and transformation (Sambrook and Russell 2001). Conjugations involving *R. leguminosarum* strains were performed as previously described (Finan *et al.* 1985). NCBI Primer BLAST, NEBuilder, and SnapGene Viewer were used for designing cloning primers (Ye *et al.* 2012; New England Biolabs; GSL Biotech LLC). All constructs made in this work were confirmed by sequencing. Nucleotide sequencing was outsourced through Manitoba Institute of Cell Biology Sequencing Service and Génome Québec.

2.3 Inverse PCR for the Construction of Rlt278 and Rlt279

The following method was used to generate *rhaT* partial deletion mutants. The gene of interest, *rhaT*, was PCR amplified and cloned into a high copy number plasmid (pBlueScript II SK). Using primers targeting the internal region of the gene (Table 2), nearly everything including the vector backbone was amplified using Q5 High Fidelity polymerase from NEB. A high fidelity commercial polymerase is recommended in order to minimize errors during this long PCR amplification. The end result is a linear fragment of the vector backbone flanked by the outer regions of *rhaT*. This linear product was ligated and essentially results in a plasmid carrying the two outer fragments of *rhaT* ligated to one another. Afterwards, this truncated *rhaT* was amplified, this time using conventional primers (Table 2). This partially deleted *rhaT* was cloned into the suicide vector pJQ200SK and then integrated into Rlt100 and Rlt144. The end

products are Rlt278 (partial *rhaT* deletion in Rlt100 background) and Rlt279 (in Rlt144 background).

2.4 Gibson Assembly Cloning

The constructs were designed on NEBuilder (a proprietary tool of New England Biolabs). For Rlt280 (full-*rhaT* deletion), 400bp fragments flanking *rhaT* were amplified. For the CUT1-like truncated *rhaT* mutants (Rlt282 and Rlt283), the desired fragment and the upstream region were amplified for a total size of 1000-bp as well as another 1000-bp fragment amplified from the vicinity of *rhaP*. The Gibson Assembly Master Mix from NEB was used for the cloning reaction. A pair of 400bp and 1000bp fragments were chosen to maximize cloning efficiency as well as allow for easy detection on a gel. Since a maximum fragment amounts of 0.5pmols were permitted for the Gibson Assembly, a larger fragment size allowed for larger input volumes. The fragment amount was calculated using the following equation: pmols = (weight in ng) x 1,000 / (base pairs x 650 daltons). The pJQ200SK vector was isolated and linearized using PstI and BamHI restriction enzymes. The Gibson Assembly reaction was performed using a thermocycler at 50°C for 1 hour. 10 µL of the reaction mix were used for transformation into DH5α.

2.5 Transport Assays

[^{3}H] radiolabelled rhamnose (5 Ci/mmol) was purchased from American Radiolabeled Ltd (St. Louis, MO). Prior to the assay, sample cultures were grown overnight in TY, then induced in defined media (VMM) supplemented with 15 mM glycerol and rhamnose. These cultures were grown to 0.5 - 0.6 OD_{600}, washed, then diluted to approximately 0.3 OD_{600} in defined

salts medium (VMM without growth factors). The rhamnose uptake assays were performed according to protocols as described (Rivers and Oresnik 2013). The sample cultures were exposed to [^{3}H] rhamnose. Most of the assays were performed using a 100:1 ratio mix of cold substrate to radiolabelled rhamnose at a final concentration of 2 µM. Assays were conducted over 1 minute with a data point every 20 seconds, 3 minutes (read every minute), to an hour (with data points at 1 minute, 15 minutes, 30, and 60 minutes). At corresponding time points, 500 µL of the culture was pipetted onto a 0.45 µm Millipore HV filter on a Millipore vacuum manifold. 5mL of defined salts medium was inputted directly after sample deployment to wash away unincorporated [^{3}H] label. The filters were placed into sample vials containing scintillation fluid. Each sample was measured on a Beckman Coulter LS6500 Liquid Scintillation Counter using the pre-set protocol "TRITIUM" for 1 minute.

2.6 Growth Curves

Each replicate was grown as an independent culture overnight in TY. These cultures were sub-cultured and grown to mid-log phase, then aliquoted into a 96-well plate. In every run, the top half (rows A, B, C, and D) was dedicated for VMM glucose samples. The bottom half (E, F, G, H) was reserved for VMM rhamnose samples. The growth kinetics were monitored using a BioTek Epoch Microplate Spectrophotometer. The programmed protocol maintained a consistently gentle shaking and measured OD_{600} every hour for 72 hours. The resulting data were collected and organized using BioTek Gen5 Data Analysis Software.

2.7 Bioinformatic Analysis

Basic local alignment was performed using the NCBI BLAST suite (Altschul *et al.* 1990). Following BLASTp, preliminary predictions of conserved domains were determined by the Conserved Domain Database (CDD) (Marchler-Bauer *et al.* 2017). Multiple sequence alignment of ABC proteins was performed using PRALINE (Simossis and Heringa 2005). On PRALINE, PSI-BLAST algorithm was used to align the queries, which were scored using BLOSUM62 exchange matrix. Predicted structures of truncated RhaT variants and their CUT1 reference ABC proteins were generated using Protein Homology / Analogy Recognition Engine (Phyre) 2 with "Intensive" modelling (Kelley *et al.* 2015). These .PDB files were visualized on PyMOL Open Source v1.8 by Schrödinger LLC.

Chapter 3:

Results

3.1 Investigation of RhaK-RhaT interaction using *rhaT* deletion mutants

Physical interaction between the sugar kinase RhaK and rhamnose ABC importer ATPase RhaT was discovered in a previous work (Rivers and Oresnik 2015). In that work, the region of interaction in RhaK was determined as alleles RhaK72 and RhaK73. This thesis initially began with the intent of continuing the work on the RhaK-RhaT interaction by determining the region of interaction in RhaT. A *rhaT* deletion was made in Rlt100 using a deletion technique termed inverse PCR, which amplifies an isolated gene on a plasmid where the reverse primer targets an upstream region and the forward primer on the downstream region. The end result of this method is a partial deletion of the gene, amplifying all but the inner fragment of the target gene (Figure 3). This deletion was made in both wildtype (Rlt100) and *rhaK*::Tn*5* (Rlt144) strain backgrounds. These strains were constructed in order to generate *rhaT* $^{-}$ and *rhaT* $^{-}$*rhaK* $^{-}$ double mutant backgrounds to engineer the RhaK-RhaT interaction using modified variants.

These partial deletion mutants exhibited growth on rhamnose as a sole carbon source, albeit at a reduced rate. To minimize the rhamnose transport background noise during subsequent experiments, a full *rhaT* deletion mutant was generated. This mutant was designed and cloned into *E. coli* DH5α using Gibson assembly cloning, then integrated into *R. leguminosarum* to generate the deletion. The basis of this construction was amplifying 400bp of the regions flanking *rhaT*, then using those flanks to recombine into the genome and delete *rhaT*.

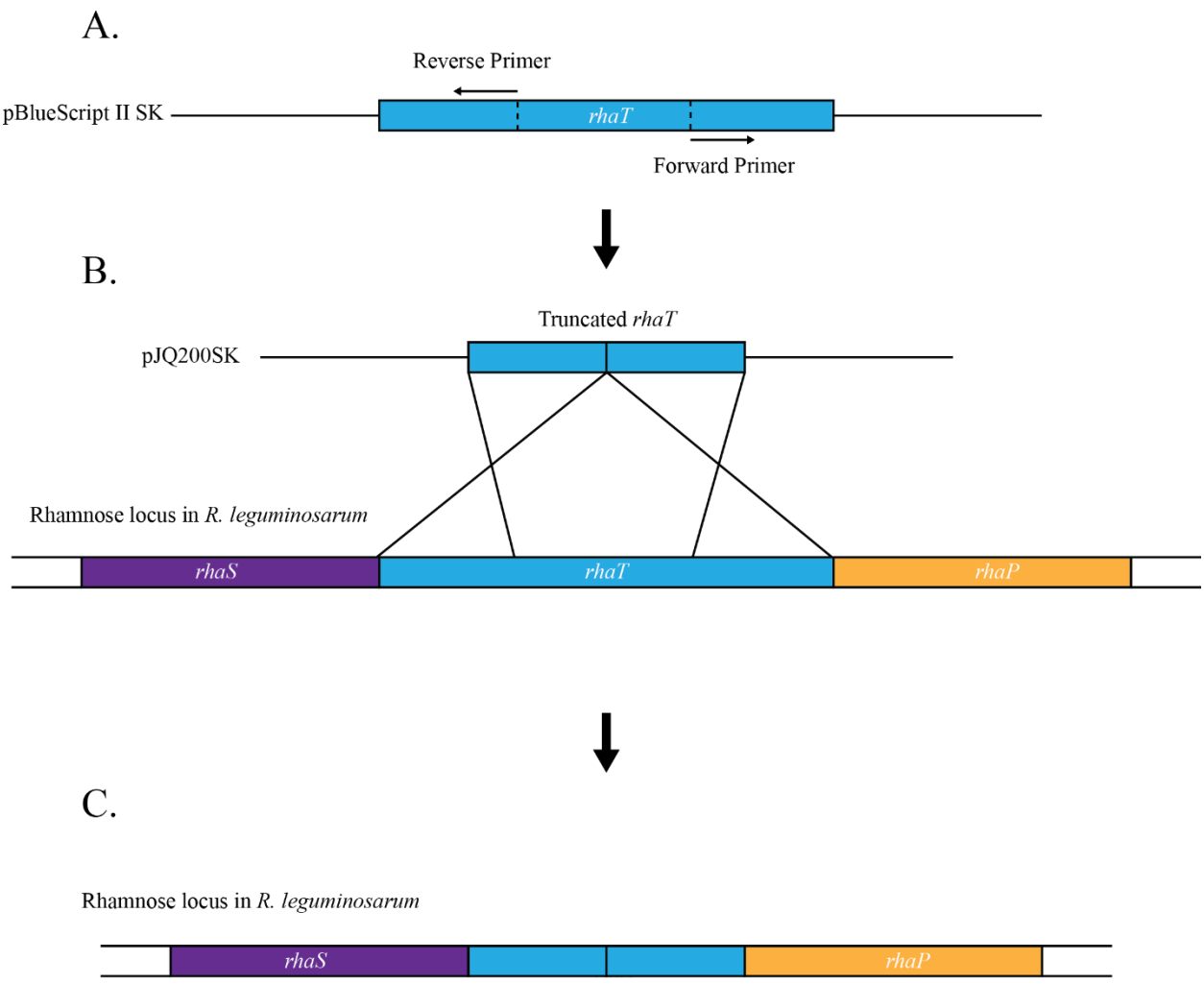

Figure 3. Construction of the truncated *rhaT* (Rlt278) using inverse PCR.

Each line indicates a circular strand of DNA presented in linear form for simplicity. The box within the dashed lines represent the portion of *rhaT* that have been deleted. (A) After cloning *rhaT* onto a cloning plasmid (pBluescript), reverse PCR amplifies all except the internal region of *rhaT*. The product is ligated to form a circular plasmid carrying the truncated gene. (B) Truncated *rhaT* is amplified, cloned into a suicide vector, then conjugated into *R. leguminosarum* and recombined into the genome, resulting in Rlt278 (C).

3.2 RhaT is unable to be complemented on a plasmid.

Complementation experiments yielded successful complementation of *rhaK* and restored its associated phenotypes using *rhaK* expressed in the pRK7813 vector (pMR110) (Richardson and Oresnik 2007). However, the deletion of *rhaT* could not be complemented in any *R. leguminosarum rhaT* mutant using a single gene expressed in pRK7813 (pDR197) (Table 3). This was hypothesized to be due to *rhaT* being unable to be expressed properly as a single gene as it is meant to be assembled as a complex of membrane proteins along with the rest of the rhamnose transporter machinery in the operon simultaneously. In contrast, *rhaK* is a sugar kinase which stands as an independent protein. This resulted in a shift in the direction of the investigation as well as the usage of the aforementioned *rhaT* deletion strains.

Table 3. Complementation of *rhaT* deletion strains.

Strain[c]	Relevant Genotype	VMM Glc[a]	VMM Rha[a]	TYSmTc[ab]	TY[a]
Rlt100	Wild-type	++	++	-	++
Rlt278	Partial Δ*rhaT* in Rlt100	++	+	-	++
Rlt278 pDR197	*rhaT* in pRK7813	++	+	++	++
Rlt280	Full Δ*rhaT* in Rlt100	++	-	-	++
Rlt280 pDR197	*rhaT* in pRK7813	++	-	++	++
Rlt144	*rhaK*::Tn*5* in Rlt100	++	-	-	++
Rlt144 pMR110	*rhaK* in pRK7813	++	++	++	++

[a] ++ indicates robust growth comparable to wildtype, + for slow growth, and - for no growth.
[b] All complementation plasmids were constructed in a pRK7813 plasmid backbone, which confers tetracycline (Tc) resistance.
[c] pDR series plasmids were constructed in Rivers and Oresnik 2013 and pMR110 in Richardson and Oresnik 2007.

3.3 Slow growing phenotype of the truncated RhaT in Rlt278.

Despite the deletion mutants being unable to be used for their intended purpose, an unexpected phenotype was discovered in the partial deletion mutants. The *rhaT* deletion mutant in the Rlt100 background, Rlt278, exhibited a slow growth phenotype in defined media supplemented with rhamnose as a sole carbon source (Figure 4). The growth rate of this strain is 11.8 hours per generation, which is two times slower than the wildtype (Table 4). Rlt243, generated in Richardson *et al*. 2008, was used as a reference strain for slow-growth phenotype. Rlt278 showed comparable growth rates to Rlt243, at 11.8 hours to 11.6 hours, respectively. This growth was also dependent on RhaK, as the same partial *rhaT* deletion in the *rhaK* knockout strain (Rlt279) did not exhibit any growth (Table 4). This confirms that this strain is growing due to rhamnose being taken up, rather than growing using unrelated substances such as agar.

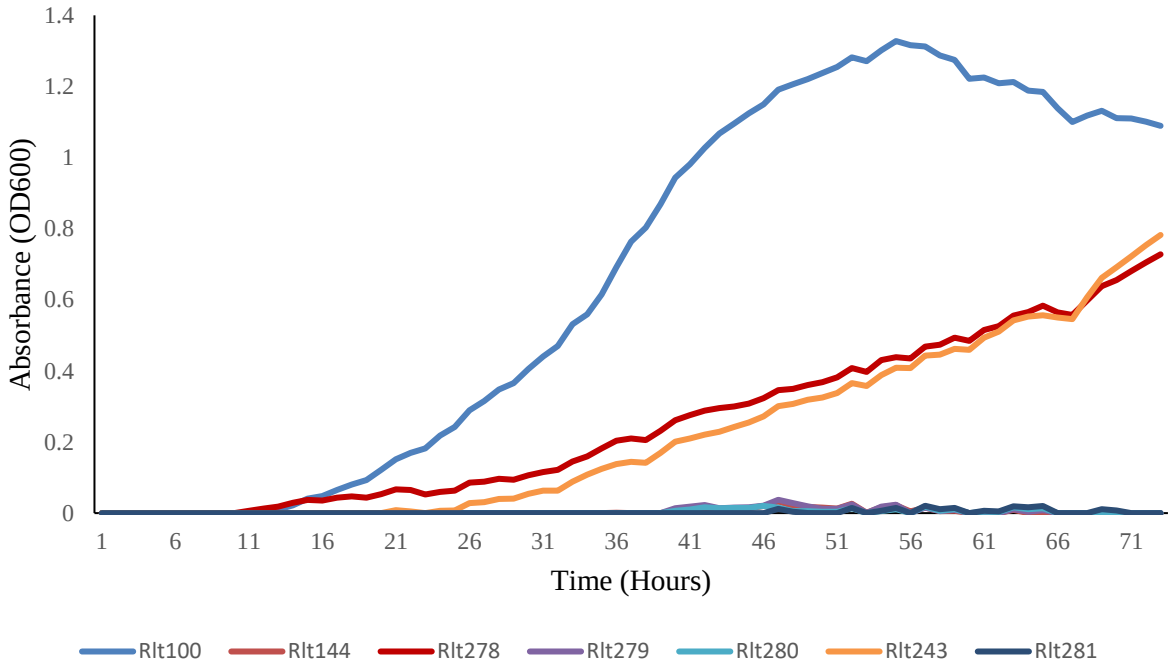

Figure 4. Growth rates of *rhaT* deletion mutants.

All data points were subtracted by blank (VMM) control cells. The samples were grown in a defined medium supplemented with 15 mM rhamnose.

Table 4. Generation time of rhamnose locus mutants.

Strain	Relevant Genotypes	Generation Time (Hours)[a]
Rlt100	Wild-type	5.92 ± 0.03
Rlt144	*rhaK*::Tn*5*	NG[b]
Rlt278	Partial Δ*rhaT* in Rlt100	11.8 ± 0.05
Rlt279	Partial Δ*rhaT rhaK*::Tn*5*	NG[b]
Rlt280	Δ*rhaT* in Rlt100	NG[b]
Rlt243	Δ*rhaU* in Rlt100	11.6 ± 0.1
Rlt281	Partial Δ*rhaT* with NBD2 removed	NG[b]

[a] Generation times and standard deviations were calculated from 5 independent replicates. Generation times were calculated using the equation Time / ((log ($OD_{600final}$) – log ($OD_{600initial}$)) / log 2). The initial OD_{600} was 0.01 for all samples and the final OD_{600} was selected from the final datapoint of log-phase growth on the growth curve.

[b] No growth; attempts at calculating generation time resulted in log0, negative values, or > 32 hours.

3.4 Analysis of the truncated *rhaT* in Rlt278

A preliminary analysis of the truncated *rhaT* sequence showed that residues 1 - 213 and 365 - 512 remained, and the region termed *rhaT*F1, previously determined to interact with RhaK (Rivers and Oresnik 2015) was left intact due to an oversight during the construction process. While the presence of this region disqualifies this strain from its original intended use, this construct proved to be a curiosity which gave insights to the minimal requirements for an ABC importer to function and the relationship between the different types within the prominent classification system in carbohydrate importers. In order to determine the mechanism responsible for the preservation of RhaT activity, the sequence was compared to consensus sequences on local alignment software, namely BLASTp and Praline (Altschul *et al.* 1990; Simossis and Heringa 2005; Marchler-Bauer *et al.* 2017).

In ABC carbohydrate importers, there is a classification system that distinguishes between two groups by the ATP-binding Cassette (ABC) structure (Schneider 2001). Carbohydrate Uptake Transporter 1 (CUT1) importers possess two copies of the nucleotide binding domain, encoded by a single gene. In contrast, CUT2 transporters such as the rhamnose transporter have a larger gene that encodes a single ABC protein with two nucleotide binding domains (NBDs), each possessing a complete set of motifs found in CUT1 ABCs. Local alignment showed that this partial deletion left the majority of its NBD1 intact (Figure 5). Of the conserved ABC motifs, only the Switch domain / H-loop was removed from the first NBD. However, the H-loop has empirically been shown to be essential for NBD activity (Zaitseva *et al.* 2005). In NBD2, the P-loop / Walker A and Q-loop are missing. These motifs are responsible for the binding of ATP and serve as a contact point for the transmembrane domain, respectively.



Figure 5. Amino acid sequence of the truncated RhaT in Rlt278.

The motifs are labelled directly above the corresponding sequence. The region deleted from the wild-type is displayed in red.

In CUT2 ABC proteins, there is a substitution of the conserved lysine to an arginine in the P-loop (GXXGXGKS/T). This substitution is believed to prohibit ATP-binding, rendering the second P-loop a vestige of an ancient fusion between two ABCs (Schneider 2001). A modified partial deletion strain (Rlt281) was constructed to determine if the truncated RhaT was capable of functioning with solely NBD1 preserved. However, Rlt281 was incapable of growing on rhamnose, suggesting that both portions of the NBDs are required for this truncated hybrid ABC to function properly (Table 4). The lack of P-loop and Q-loop in NBD2 makes it unlikely that both NBDs are functioning via the same mechanism as the wild-type. This led to the hypothesis that this protein is working as a single NBD domain. In a typical NBD, there is a helical region between Walker A and Walker B motifs. With the omission of the upstream region of NBD2, the P-loop could potentially orient itself towards the Walker B motif of the second NBD rather than the first, forming a longer helix than what it would normally possess and appropriate the remainder of NBD2 as NBD1.

3.5 Designing a CUT1 rhamnose ABC protein

To validate the single NBD hypothesis, the focus shifted towards designing a truncated variant of RhaT that functions with only one NBD. This would essentially convert the rhamnose transporter into a CUT1 importer. To maximize the likelihood of this conversion, the sequence of RhaT was compared to various CUT1 ABCs from *Sinorhizobium meliloti* 1021 as well as the most representative member of CUT1, MalK from the *Escherichia coli* K-12 maltose transporter. Although *Sinorhizobium meliloti* is somewhat phylogenetically distant from *Rhizobium leguminosarum*, both organisms feature a large number of ABC importers to thrive in the rhizosphere and engage in symbiotic interactions (Mauchline *et al.* 2006). The rhamnose

transporters in both organisms also share close similarities. The dedicated genetic database (http://iant.toulouse.inra.fr/S.meliloti) and its associated tools made *Sinorhizobium meliloti* the most appealing species when it came to selecting a number of similar genes for analysis.

Truncated RhaT from Rlt278 was aligned to 7 CUT1 sequences (Figure 6). This alignment supported the plausibility of the truncated RhaT behaving as a CUT1-like NBD. Despite the similarities, there were some key differences in motif sequences. The main difference was that CUT2 proteins do not have identical sequences for the core motifs between the two NBDs. As previously noted, the P-loop of NBD2 has an arginine substitution in place of a conserved lysine. NBD2 ABC signature motif has the characteristic "LSGGQ" sequence but in contrast, the signature motif in NBD1 has less conservation with the exception of the final glutamine. In addition, the NCBI Conserved Domain Database (CDD) revealed different families with distinct sequence architecture within CUT1 ABCs. Quintessential CUT1 examples such as the *E. coli* MalK and similar ABCs belong to a family annotated as "PRK11000" or "MalK" on the CDD. These ABC proteins have most of their conserved core motifs situated in the first half of the peptide and the C-terminal region (~100 AA) appears to be solely dedicated to the regulatory domain (Figure 7). There is another group of CUT1 ABCs such as the Fructose transporter FrcA from *Sinorhizobium meliloti*, which is listed as a member of the "MglA" family. Unlike MalK, motifs in FrcA are spread out across the peptide and it does not appear to possess a regulatory region. A multiple sequence alignment between the two proteins accentuate the differences. The most notable differences are the position of where the p-loop begins, the spacing in between Walker A and ABC signature motif, and the region downstream of the H-loop, presumably due due to the presence of a C-terminal regulatory domain in MalK (Figure 6). The lack of a regulatory region results in MglA ABCs being around 80-100 AA shorter than MalK

ABCs. Interestingly, RhaT is annotated as a MglA member even though it is a CUT2 ABC. Despite this, comparison of the motif layouts between RhaT and FrcA revealed a near-identical layout (Figure 7). For this reason, FrcA was used as a model for constructing the CUT1-like truncated RhaT.

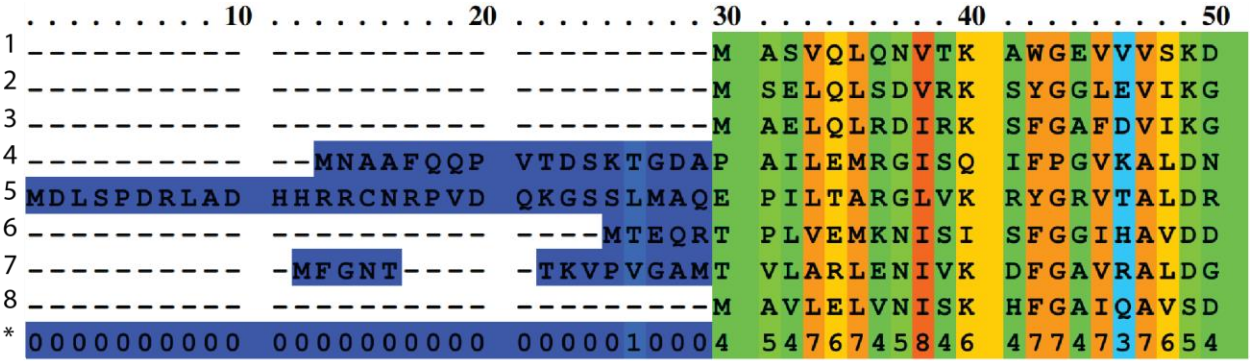
. . . . . 10 . . . . . 20 . . . . . 30 . . . . . 40 50
1 ---------- ---------- ---------M ASVQLQNVTK AWGEVVVSKD
2 ---------- ---------- ---------M SELQLSDVRK SYGGLEVIKG
3 ---------- ---------- ---------M AELQLRDIRK SFGAFDVIKG
4 ---------- --MNAAFQQP VTDSKTGDAP AILEMRGISQ IFPGVKALDN
5 MDLSPDRLAD HHRRCNRPVD QKGSSLMAQE PILTARGLVK RYGRVTALDR
6 ---------- ---------- ----MTEQRT PLVEMKNISI SFGGIHAVDD
7 ---------- -MFGNT---- -TKVPVGAMT VLARLENIVK DFGAVRALDG
8 ---------- ---------- ---------M AVLELVNISK HFGAIQAVSD
* 0000000000 0000000000 0000010004 5476745846 4774737654

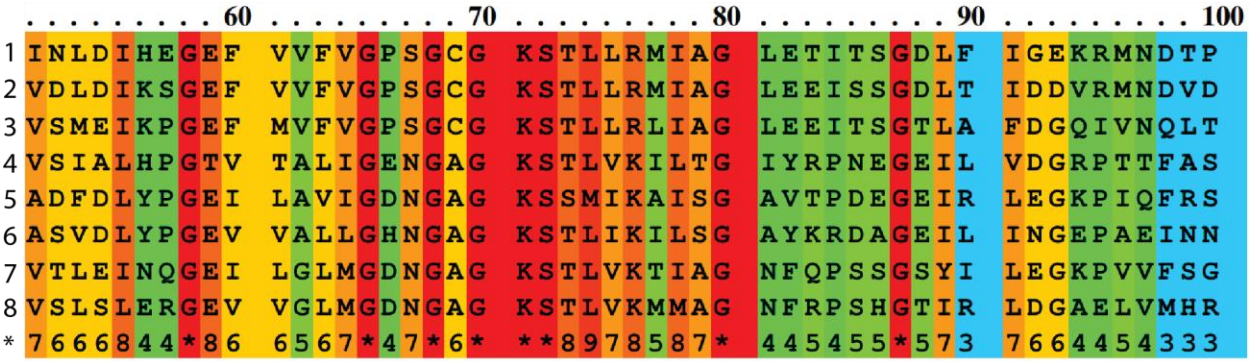
. . . . . 60 . . . . . 70 . . . . . 80 . . . . . 90 100
1 INLDIHEGEF VVFVGPSGCG KSTLLRMIAG LETITSGDLF IGEKRMNDTP
2 VDLDIKSGEF VVFVGPSGCG KSTLLRMIAG LEEISSGDLT IDDVRMNDVD
3 VSMEIKPGEF MVFVGPSGCG KSTLLRLIAG LEEITSGTLA FDGQIVNQLT
4 VSIALHPGTV TALIGENGAG KSTLVKILTG IYRPNEGEIL VDGRPTTFAS
5 ADFDLYPGEI LAVIGDNGAG KSSMIKAISG AVTPDEGEIR LEGKPIQFRS
6 ASVDLYPGEV VALLGHNGAG KSTLIKILSG AYKRDAGEIL INGEPAEINN
7 VTLEINQGEI LGLMGDNGAG KSTLVKTIAG NFQPSSGSYI LEGKPVVFSG
8 VSLSLERGEV VGLMGDNGAG KSTLVKMMAG NFRPSHGTIR LDGAELVMHR
* 7666844*86 6567*47*6* **8978587* 445455*573 7664454333

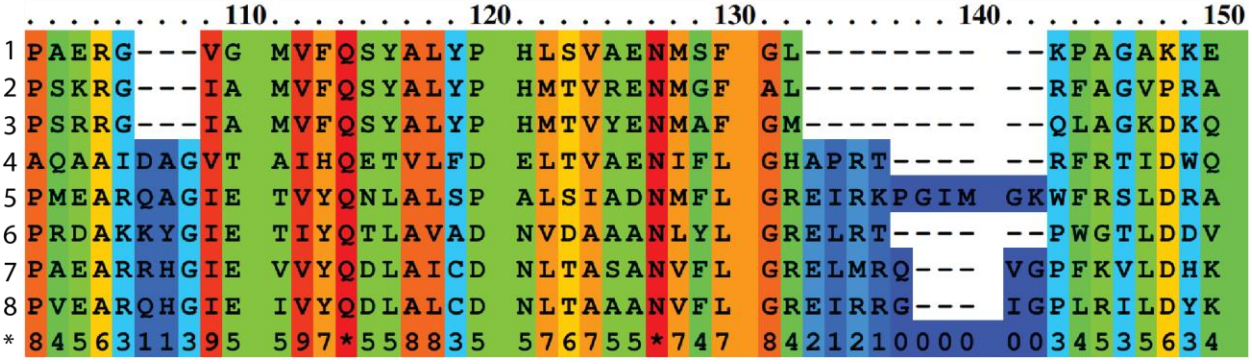
. . . . . 110 . . . . . 120 . . . . . 130 . . . . . 140 150
1 PAERG---VG MVFQSYALYP HLSVAENMSF GL-------- --KPAGAKKE
2 PSKRG---IA MVFQSYALYP HMTVRENMGF AL-------- --RFAGVPRA
3 PSRRG---IA MVFQSYALYP HMTVYENMAF GM-------- --QLAGKDKQ
4 AQAAIDAGVT AIHQETVLFD ELTVAENIFL GHAPRT---- --RFRTIDWQ
5 PMEARQAGIE TVYQNLALSP ALSIADNMFL GREIRKPGIM GKWFRSLDRA
6 PRDAKKYGIE TIYQTLAVAD NVDAAANLYL GRELRT---- --PWGTLDDV
7 PAEARRHGIE VVYQDLAICD NLTASANVFL GRELMRQ--- VGPFKVLDHK
8 PVEARQHGIE IVYQDLALCD NLTAAANVFL GREIRRG--- IGPLRILDYK
* 8456311395 597*558835 576755*747 8421210000 0034535634

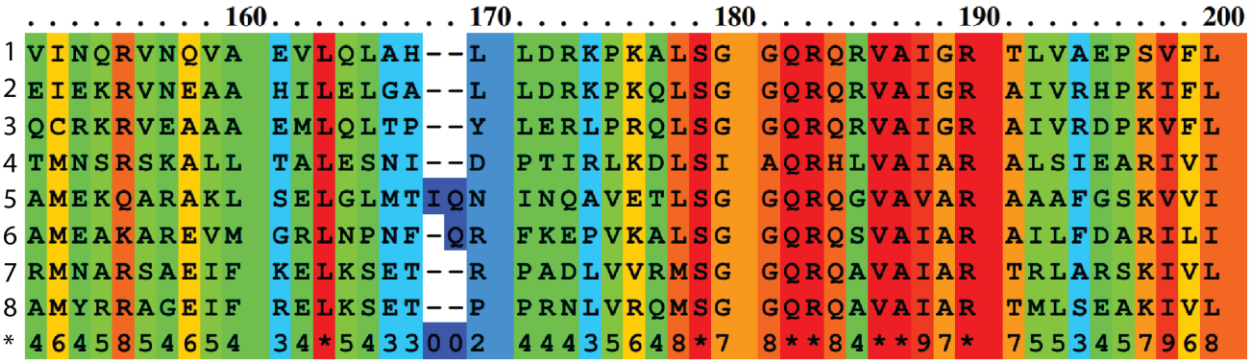
. . . . . 160 . . . . . 170 . . . . . 180 . . . . . 190 200
1 VINQRVNQVA EVLQLAH--L LDRKPKALSG GQRQRVAIGR TLVAEPSVFL
2 EIEKRVNEAA HILELGA--L LDRKPKQLSG GQRQRVAIGR AIVRHPKIFL
3 QCRKRVEAAA EMLQLTP--Y LERLPRQLSG GQRQRVAIGR AIVRDPKVFL
4 TMNSRSKALL TALESNI--D PTIRLKDLSI AQRHLVAIAR ALSIEARIVI
5 AMEKQARAKL SELGLMTIQN INQAVETLSG GQRQGVAVAR AAAFGSKVVI
6 AMEAKAREVM GRLNPNF-QR FKEPVKALSG GQRQSVAIAR AILFDARILI
7 RMNARSAEIF KELKSET--R PADLVVRMSG GQRQAVAIAR TRLARSKIVL
8 AMYRRAGEIF RELKSET--P PRNLVRQMSG GQRQAVAIAR TMLSEAKIVL
* 4645854654 34*5433002 4443564 8*7 8**84**97* 7553457968

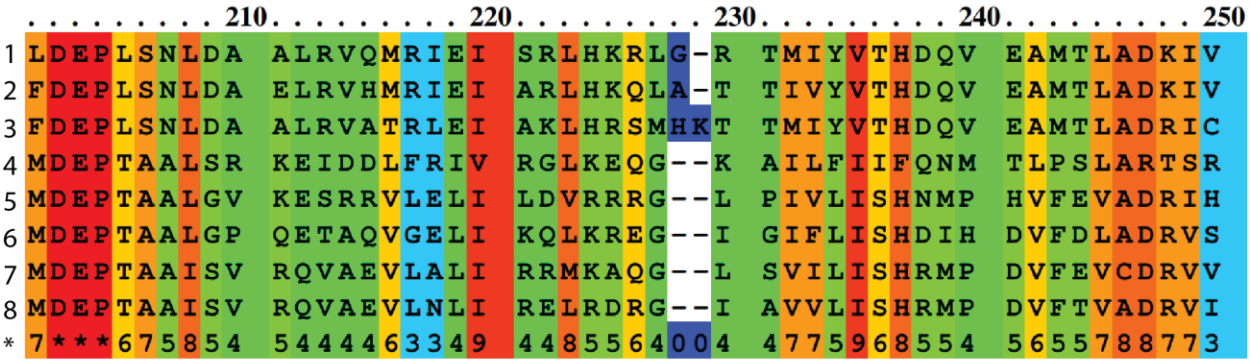
. . . . . 210 . . . . . 220 . . . . . 230 . . . . . 240 250
1 LDEPLSNLDA ALRVQMRIEI SRLHKRLG-R TMIYVTHDQV EAMTLADKIV
2 FDEPLSNLDA ELRVHMRIEI ARLHKQLA-T TIVYVTHDQV EAMTLADKIV
3 FDEPLSNLDA ALRVATRLEI AKLHRSMHKT TMIYVTHDQV EAMTLADRIC
4 MDEPTAALSR KEIDDLFRIV RGLKEQG--K AILFIIFQNM TLPSLARTSR
5 MDEPTAALGV KESRRVLELI LDVRRRG--L PIVLISHNMP HVFEVADRIH
6 MDEPTAALGP QETAQVGELI KQLKREG--I GIFLISHDIH DVFDLADRVS
7 MDEPTAAISV RQVAEVLALI RRMKAQG--L SVILISHRMP DVFEVCDRVV
8 MDEPTAAISV RQVAEVLNLI RELRDRG--I AVVLISHRMP DVFTVADRVI
* 7***675854 5444463349 4485564004 4775968554 5655788773

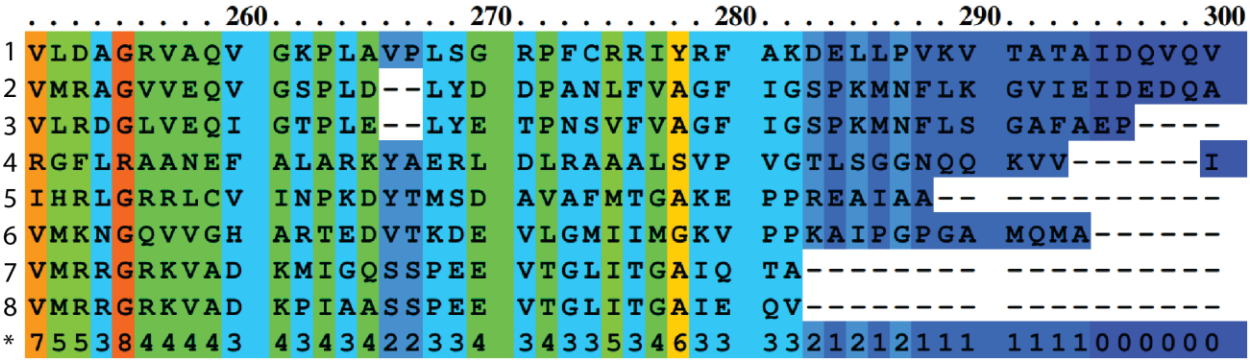
. . . . . 260 . . . . . 270 . . . . . 280 . . . . . 290 300
1 VLDAGRVAQV GKPLAVPLSG RPFCRRIYRF AKDELLPVKV TATAIDQVQV
2 VMRAGVVEQV GSPLD--LYD DPANLFVAGF IGSPKMNFLK GVIEIDEDQA
3 VLRDGLVEQI GTPLE--LYE TPNSVFVAGF IGSPKMNFLS GAFAEP----
4 RGFLRAANEF ALARKYAERL DLRAAALSVP VGTLSGGNQQ KVV------I
5 IHRLGRRLCV INPKDYTMSD AVAFMTGAKE PPREAIAA-- ----------
6 VMKNGQVVGH ARTEDVTKDE VLGMIIMGKV PPKAIPGPGA MQMA------
7 VMRRGRKVAD KMIGQSSPEE VTGLITGAIQ TA-------- ----------
8 VMRRGRKVAD KPIAASSPEE VTGLITGAIE QV-------- ----------
* 7553844443 4343422334 3433534633 3321212111 1111000000

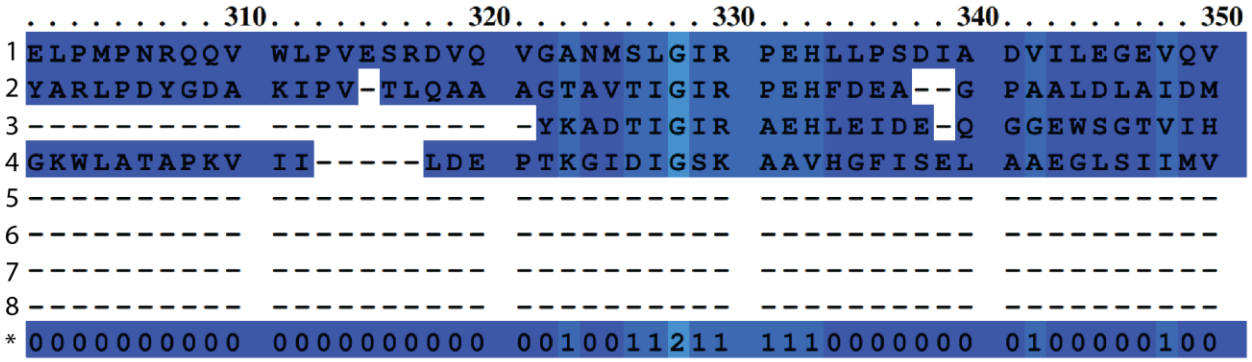
. . . . . 310 . . . . . 320 . . . . . 330 . . . . . 340 350
1 ELPMPNRQQV WLPVESRDVQ VGANMSLGIR PEHLLPSDIA DVILEGEVQV
2 YARLPDYGDA KIPV-TLQAA AGTAVTIGIR PEHFDEA--G PAALDLAIDM
3 ---------- ---------- -YKADTIGIR AEHLEIDE-Q GGEWSGTVIH
4 GKWLATAPKV II-----LDE PTKGIDIGSK AAVHGFISEL AAEGLSIIMV
5 ---------- ---------- ---------- ---------- ----------
6 ---------- ---------- ---------- ---------- ----------
7 ---------- ---------- ---------- ---------- ----------
8 ---------- ---------- ---------- ---------- ----------
* 0000000000 0000000000 0010011211 1110000000 0100000100

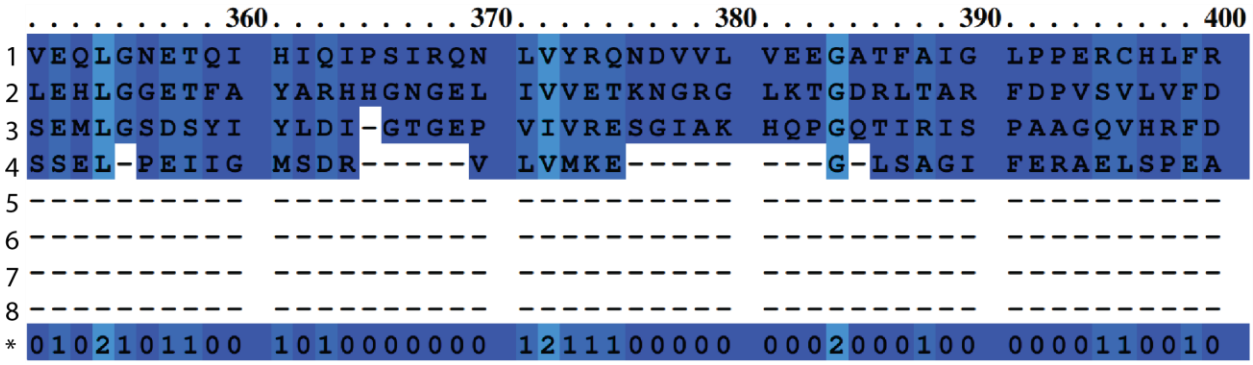
. . . . . 360 . . . . . 370 . . . . . 380 . . . . . 390 400
1 VEQLGNETQI HIQIPSIRQN LVYRQNDVVL VEEGATFAIG LPPERCHLFR
2 LEHLGGETFA YARHHGNGEL IVVETKNGRG LKTGDRLTAR FDPVSVLVFD
3 SEMLGSDSYI YLDI-GTGEP VIVRESGIAK HQPGQTIRIS PAAGQVHRFD
4 SSEL-PEIIG MSDR-----V LVMKE----- ---G-LSAGI FERAELSPEA
5 ---------- ---------- ---------- ---------- ----------
6 ---------- ---------- ---------- ---------- ----------
7 ---------- ---------- ---------- ---------- ----------
8 ---------- ---------- ---------- ---------- ----------
* 0102101100 1010000000 1211100000 0002000100 0000110010

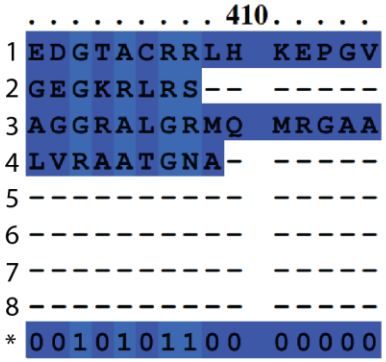
. . . . . 410 . . . .
1 EDGTACRRLH KEPGV
2 GEGKRLRS-- -----
3 AGGRALGRMQ MRGAA
4 LVRAATGNA- -----
5 ---------- -----
6 ---------- -----
7 ---------- -----
8 ---------- -----
* 0010101100 00000

Figure 6. Multiple sequence alignment of CUT1 ABC proteins and truncated RhaT. Modified from PRALINE sequence alignment results summary. * indicates the conservation score for the corresponding residues on a scale of 0 to 10 based on the BLOSUM62 matrix. These numbers are colour-coded to visualize the degree of conservation. The numbers to the left of the alignment represent the following query samples: (1) *E. coli* MalK; (2) *S. meliloti* LacK; (3) *S. meliloti* ThuK; (4) *R. leguminosarum* Rlt278 truncated RhaT; (5) *S. meliloti* FrcA; (6) *S. meliloti* SMb20904; (7) *S. meliloti* SMc03815; (8) *S. meliloti* SMb20930.

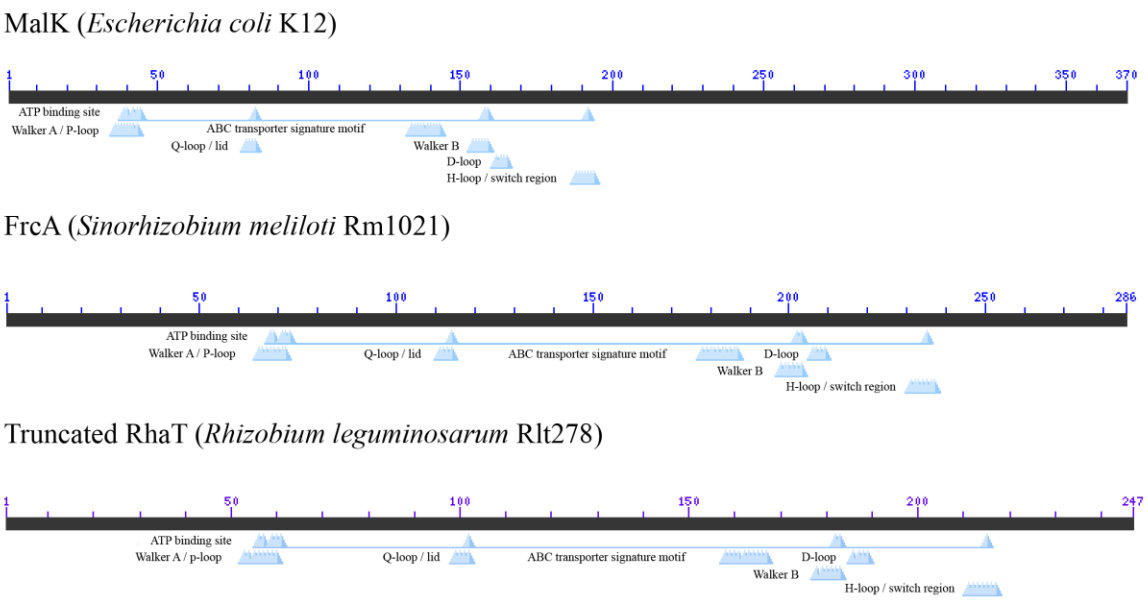

Figure 7. Motif layouts of CUT1 ABCs and the truncated RhaT.

Modified from BLASTp Conserved Domain Database (Marchler-Bauer *et al.* 2017). A ~250AA RhaT segment (containing only NBD1) from Rlt100 was used for this analysis.

3.6 Determination of a truncation site

The optimal site of truncation was selected based on the criteria of ensuring that it maintains the same structure and theoretically shows promise of proper activity. The area of interest for this question is the variable region in between NBD1 and NBD2 in RhaT. Between the H-loop of NBD1 and the p-loop of NBD2, there is a region of ~85 AA. It is unclear where NBD1 precisely ends and where NBD2 begins, therefore conserved residues were used as points of interest when considering the truncation. In the end, two sites were chosen.

The first truncation site is located immediately before the conserved sequences in NBD2, just upstream of its P-loop (Figure 8). The region between the NBDs with a relatively higher variance is preserved. The end product of this construction is a 285 AA peptide, which is consistent with the ~300 AA length observed in MglA CUT1 importers. The Phyre2 predicted model shows a folding structure similar to FrcA, but it possesses a ~20 AA stretch of a C-terminal tail without any predicted secondary structures (Figure 10). As there is no prior publication for a mutation of this nature, there were many unknown elements to consider, including whether this C-terminal region would be vital to the proper operation of the “CUT1” ABC. However, the predicted structure raised concerns about potential steric hindrances and other unforeseen outcomes.

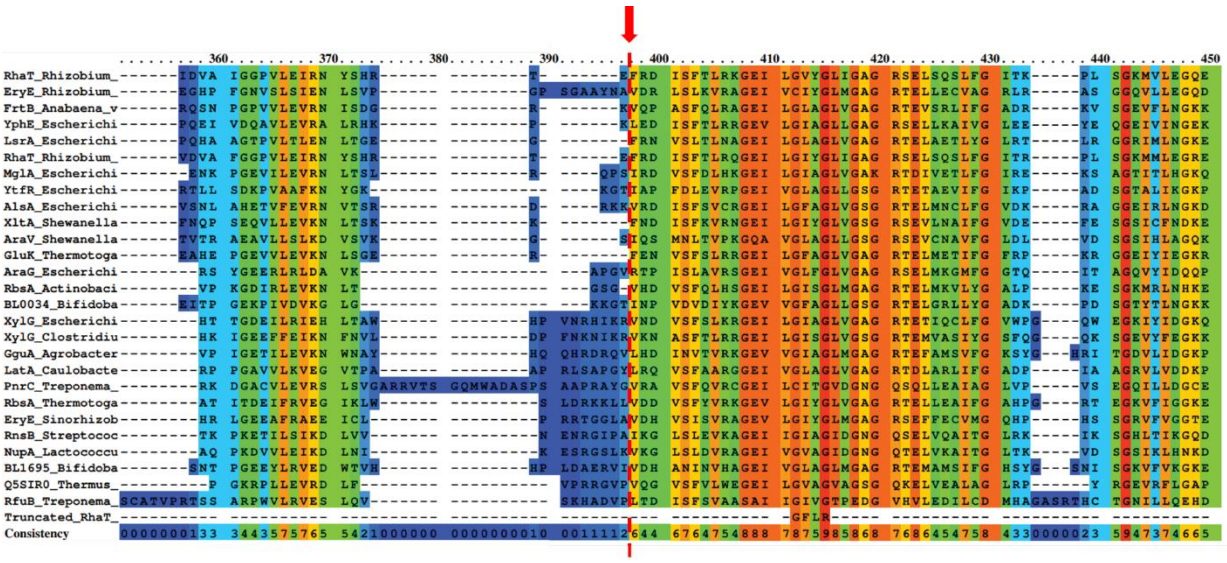

Figure 8. First truncation site of the CUT1-like *rhaT* construct.

Modified from PRALINE sequence alignment results summary. Consistency indicates the conservation score for the corresponding residues on a scale of 0 to 10 based on the BLOSUM62 matrix. These numbers are colour-coded to visualize the degree of conservation. The red arrow with the dashed lines indicates the site of truncation.

A second truncation mutant was determined to address this foldless C-terminal tail. This truncation site is located 5 AA downstream of the H-loop / Switch region, 21 AA upstream of the first site (Figure 9). The primary difference between the first and second mutant is that the latter omits the highly variable region between the NBDs. This variant of RhaT is predicted to be 264 AA. The predicted structure for this construct shows a structure identical to the 285 AA construct without the C-terminal tail (Figure 10). However, due to the lack of an unambiguous low-conservation boundary, the designation of the truncation site was somewhat subjective in nature.

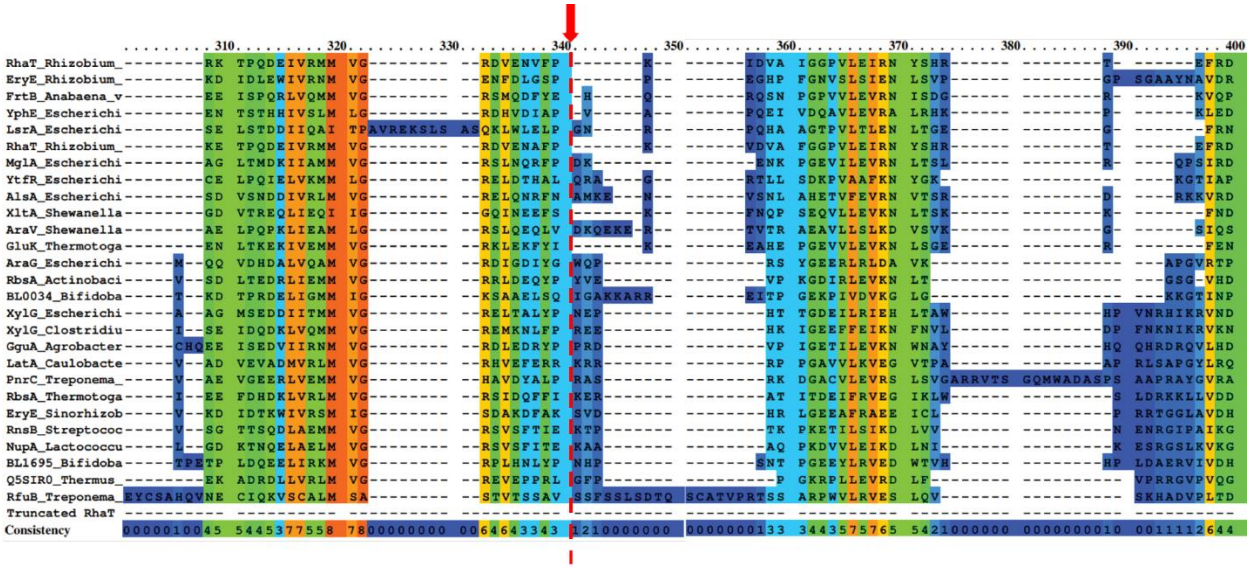

Figure 9. Second truncation site of the CUT1-like *rhaT* construct.

Modified from PRALINE sequence alignment results summary. Consistency indicates the conservation score for the corresponding residues on a scale of 0 to 10 based on the BLOSUM62 matrix. These numbers are colour-coded to visualize the degree of conservation. The red arrow with the dashed lines indicates the site of truncation.

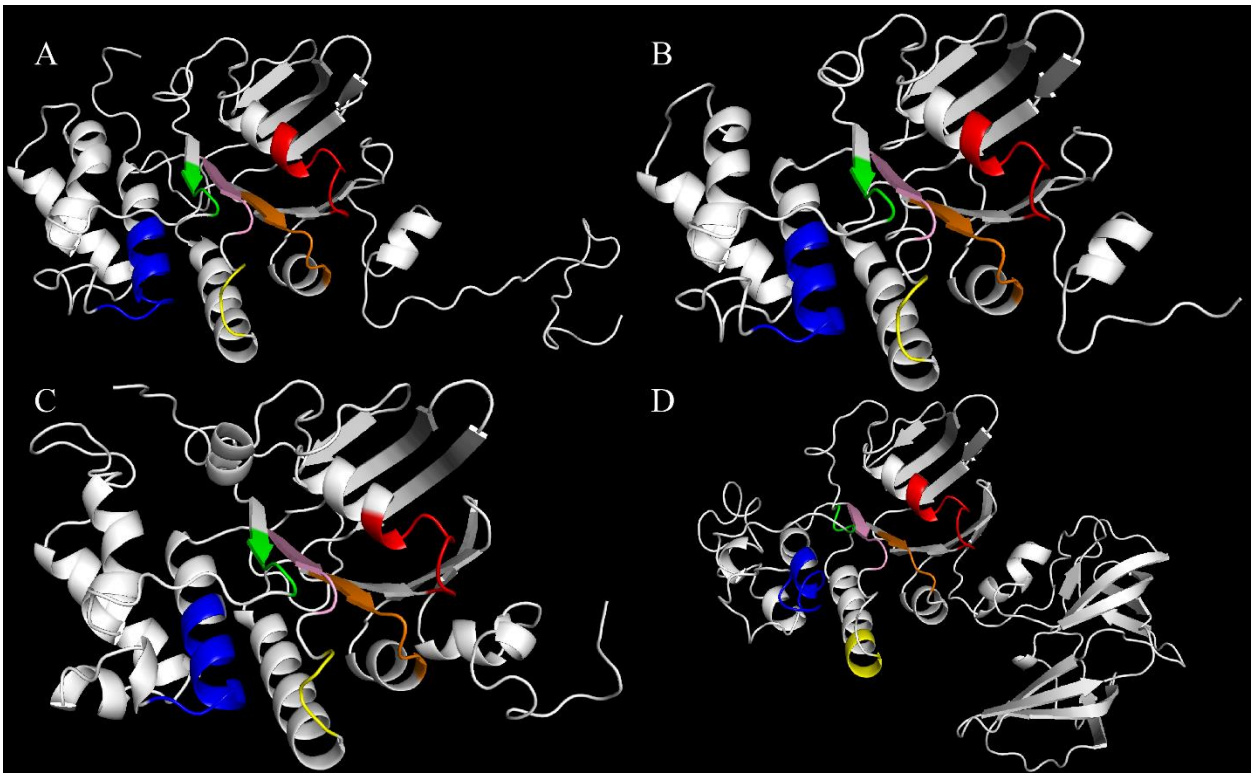

Figure 10. Predicted structure of truncated RhaT, FrcA, and MalK.

These predicted structure models were generated by Phyre2 and visualized using PyMOL. Conserved ABC motifs are represented as the following colours: P-loop / Walker A as red, Q-loop as green, ABC signature as blue, Walker B as pink, D-loop as yellow, and H-loop / Switch region as orange. (A) Predicted structure of truncated 285AA RhaT (Rlt282). (B) Predicted structure of truncated 264AA RhaT (Rlt283). (C) Predicted structure of FrcA from *Sinorhizobium meliloti* 1021. (D) Structure of MalK from *Escherichia coli* K-12 based on published crystal structure.

3.7 The truncated RhaT can utilize rhamnose as a sole carbon source.

Two variants of the truncated RhaT were cloned into pJQ200SK using Gibson assembly in *E. coli* and integrated into *Rhizobium leguminosarum* bv. *trifolii* strain Rlt100. Both Rlt282 (285AA) and Rlt283 (264AA) were shown to possess the same growth phenotype as Rlt278. Growth rates corroborate the plate phenotypes (Table 5). The fact that these independent mutations share the same phenotypes as Rlt278 suggests that the *rhaT* in Rlt278 encodes a protein which essentially function as a CUT1 NBD.

There were no significant differences in the efficiency of Rlt282 and Rlt283 in their ability to grow in rhamnose as a sole carbon source or their ability to transport the substrate. Both Rlt282 and Rlt283 had nearly the same generation times, at 12.6 and 12.3 hours, respectively. Rhamnose accumulation rates of these two strains also are not too different than that of Rlt278, though Rlt283 exhibited slightly higher rates (Figure 11). This suggests that the structure of the CUT1 NBD is not as stringent, at least in the C-terminal region or on the surface away from the face which participates in the interaction with its complementary NBD partner.

Table 5. Generation time of *rhaT* CUT1 conversion mutants.

Strain	Relevant Genotypes	Generation Time (Hours)[a]
Rlt100	Wild-type	6.55 ± 0.008
Rlt144	*rhaK*::Tn*5*	NG[b]
Rlt278	Partial Δ*rhaT* in Rlt100	12.7 ± 0.3
Rlt279	Partial Δ*rhaT rhaK*::Tn*5*	NG[b]
Rlt280	Complete Δ*rhaT* in Rlt100	NG[b]
Rlt281	Partial Δ*rhaT* with NBD2 removed	NG[b]
Rlt282	285AA *rhaT* truncation mutant	12.6 ± 0.1
Rlt283	264AA *rhaT* truncation mutant	12.3 ± 0.3

[a] Generation times and standard deviations were calculated from 4 independent replicates. Generation times were calculated using the equation Time / ((log ($OD_{600final}$) – log ($OD_{600initial}$)) / log 2). The initial OD_{600} was 0.01 for all samples and the final OD_{600} was selected from the final datapoint of log-phase growth on the growth curve.

[b] No growth; attempts at calculating generation time resulted in log0, negative values, or > 30 hours.

3.8 Accumulation of rhamnose in *rhaT* truncation mutants

To ascertain whether these strains are capable of transporting rhamnose, a radiolabelled rhamnose uptake assay was performed. The cells expressing partial *rhaT* deletion mutant (Rlt278), full deletion mutant (Rlt280), and the two CUT1-like truncation mutants (Rlt282 and Rlt283), were incubated with [^{3}H]-labelled rhamnose. This 1 minute assay yielded accumulations that were at least 1 order of magnitude lower than the wildtype, but consistently displayed slightly greater rates than the full deletion mutant (Rlt280) (Figure 11). The truncation mutants had average rates ranging between 0.17 nmol/mg/min to 0.54 nmol/mg/min, which were several times greater than Rlt280 at 0.06 nmol/mg/min (Figure 11). A repeated accumulation assay over a longer course of time displayed results which showed a larger difference between Rlt278 and Rlt280, but the rates ultimately remained low in comparison to the wild-type (Table 6). Due to the high variance in most of the samples, it is difficult to conclude that these rates are truly representative of their rhamnose uptake rates. These *rhaT* truncation strains yielded substantially lower rates of accumulation compared to Rlt243 (Δ*rhaU*), which exhibited similar growth rates (Richardson *et al.* 2008). Nevertheless, the accumulation rates are consistent with the hypothesis, though some uncertainty still remains. Although the evidence of transport is weak, the growth phenotypes strongly support the possibility that rhamnose is able to enter the cells at rates sufficient enough to sustain growth.

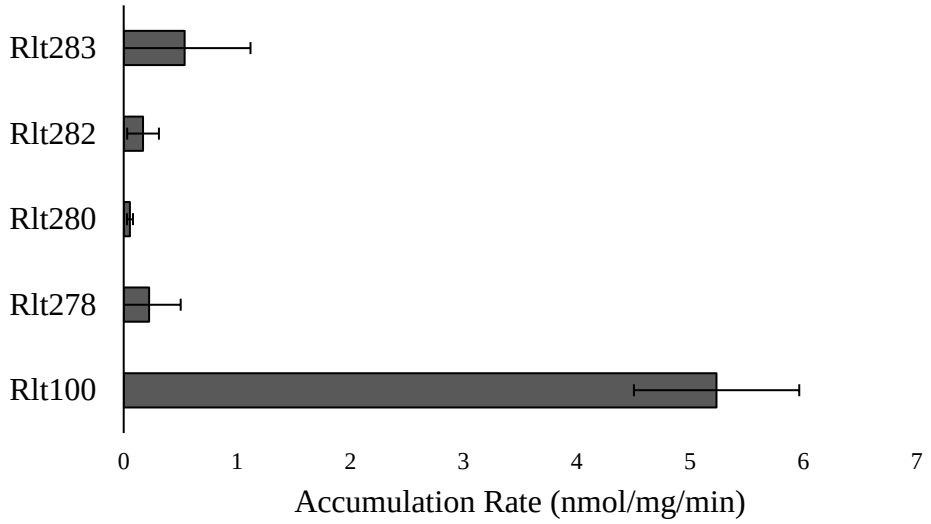

Figure 11. Accumulation of [^{3}H] L-rhamnose in *rhaT* truncation mutants over 1 minute.

All values represent averages of at least three biological replicates.

Table 6. Accumulation of rhamnose in *rhaT* deletion mutants over 1 hour.

Strain	Relevant Genotypes	Uptake Rates (nmol/mg/hr)
Rlt100	Wild-type	77.3 ± 3.2 [a]
Rlt278	Partial Δ*rhaT* in Rlt100	5.6 ± 1.5 [a]
Rlt280	Complete Δ*rhaT* in Rlt100	2.0 ± 0.6[b]

[a] Data presented are an average of three biological replicates.
b Data represents two biological replicates due to an outlier.

3.9 Complementation of *rhaT* as a polygenic transcript

The inability of *rhaT* on a plasmid to complement was hypothesized to be due to its reliance on being assembled as a complex with other constituents of the RhaSTPQ transporter. To address this roadblock, complementation was attempted using a multigene transcript. In a previous work initially characterizing the rhamnose catabolism locus, a series of transposon insertion mutants in cosmids carrying the rhamnose locus were generated (Richardson *et al.* 2004). Rhamnose locus cosmids with a transposon insertion in *rhaP*, *rhaT*, *rhaP*, or *rhaK*, were conjugated into the *rhaT* deletion strains (Table 7). *rhaP* was selected to serve as a regulatory mutant to address any changes that may occur in the absence of a negative regulator. The *rhaT* insertion was chosen as a negative control. The *rhaP* insertion disrupts the gene encoding the transmembrane permease of the transporter. This was included to determine whether only the regulator and substrate binding protein (RhaS) needed in the transcript. The *rhaK* would allow for the full expression of the transporter components and the mutarotase *rhaU*, which does not have a cosmid transposon insertion. It would also confirm whether or not *rhaK* and *rhaT* need to be expressed together in the same transcript.

Complementation was successful using the multi-gene approach. Complementation attempts using inserts in the transporter components yielded no changes, while the *rhaK* insert resulted in full complementation of *rhaT* (Table 7). This outcome was consistent across both partial and full *rhaT* deletion mutants. The restoration of the rhamnose growth phenotype was also dependent on *rhaK*, as shown by the lack of growth in the *rhaK rhaT* double mutant (Table 7).

Table 7. *rhaT* complementation in rhamnose deletion mutants using rhamnose locus cosmids carrying transposon insertions.

Strain	Relevant Genotype	TY[a]	VMM Glc[a]	VMM Rha[a]
Rlt100	Wild-type	++	++	++
Rlt278	Partial Δ*rhaT* in Rlt100	++	++	+
Rlt279	Partial Δ*rhaT rhaK*::Tn*5*	++	++	-
Rlt280	Full Δ*rhaT* in Rlt100	++	++	-
Rlt278 pW3C1	Rhamnose locus cosmid in pRK7813	++	++	++
Rlt278 pMR74	pW3C1 *rhaR*::Tn*5*	++	++	+/-[c]
Rlt278 pW3AR1	pW3C1 *rhaT*::Tn*5*	++	++	+
Rlt278 pMR67	pW3C1 *rhaP*::Tn*5*	++	++	+
Rlt278 pMR98	pW3C1 *rhaK*::Tn*5*	++	++	++
Rlt279 pMR98	pW3C1 *rhaK*::Tn*5*	++	++	-
Rlt280 pMR98	pW3C1 *rhaK*::Tn*5*	++	++	++

[a] ++ indicates robust growth comparable to wildtype, + for slow growth, and - for no growth.
[c] Peculiar patchy growth.

Chapter 4:

Discussion

This work originally began as a project to investigate the interaction between RhaT and RhaK. However, the inability to complement *rhaT* as an independent gene proved to be an obstacle. The unexpected growth phenotype of the partial deletion mutant Rlt278 (Table 4), steered the focus of this work towards another direction in characterizing the rhamnose transporter - exploring its identity as a CUT2 transporter. Until the construction of the *rhaT* truncation mutant with the NBD2 fragment removed (Rlt281), there was little to suggest that Rlt278's truncated RhaT behaves as a CUT1 ABC. The decision to pursue the investigation in this direction stemmed from realizing that there was a lack of interest in exploring CUT2. Prokaryotic ABC carbohydrate uptake transporters were last reviewed in 2001 and the CUT classification has remained stagnant ever since (Schneider 2001). Despite the lack of progress on this front, the CUT classification has seen continual use in recent characterizations of ABC importers (Pinweha *et al.* 2018; Wagner *et al.* 2018; Huang *et al.* 2019; Ravindranathan *et al.* 2019).

During the designing process of the "CUT1" RhaT truncation mutants, there were some doubts about the feasibility of this approach. For instance, the coupling helices (EAA-X_3-G-X_9-I-X-LP) that would bind NBD1 or NBD2 in the RhaSTPQ system are distinct since the permeases, RhaP and RhaQ, are heterodimers (Richardson *et al.* 2004). The literature hints that the variable region near the Q-loop could be a "barcode" with high specificity for a particular target, leading to the assumption that each EAA motif would only be compatible with its intended Q-loop partner (Schmitt *et al.* 2003). This raised concerns about whether or not a copy of NBD1 would be able to bind the coupling helix that would typically bind the Q-loop in NBD2. However, the truncation products were able to function properly, suggesting that the EAA motifs are less

stringent than assumed. This raised a new set of questions. How would it be possible for the transporter to ensure that the transporter complex is assembled in the correct orientation and prevent the NBDs of one transporter from binding to permeases of another transporter? Perhaps this is why the members of the transporter complex must be transcribed together. An interesting avenue to explore in the future would be to attempt constructing a CUT2 from a CUT1 transporter. Though it is likely to be far more challenging than truncating a CUT2 ABC to form a CUT1, this construction may reveal some characteristics of each type that would not have been found otherwise. This can also attempt to answer some questions about EAA compatibility.

All of the truncated RhaTs were incapable of showing linear rhamnose transport kinetics in our assays (Figure 12). For longer accumulation assays, there were many samples that showed a net decrease of radiolabelled rhamnose in the cell. The inability to exhibit a linear increase of rhamnose accumulation in the *rhaT* truncation mutants prompted trials with increasing ratios of radiolabelled rhamnose to unlabelled substrate but resulted in negligible changes. With consistent evidence of growth on rhamnose as a sole carbon source in both broth cultures and agar plates, it is rather unlikely that there is no transport whatsoever. However, it is undeniable that there were no detectable rates that could be resolved by increasing the concentration of radiolabeled substrate. Although there is no conclusive evidence to support this, it may be possible that this phenomenon is primarily due to a decreased uptake performance by the transporter. It is likely that this truncated transporter is suboptimal compared to wildtype as it is a truncation product since one of the NBD does not possess the proper sequences that has been optimized for that particular system. If this is the case, it may have led to a rate of transport which could not substantially exceed the rate of catabolism, whereas the wildtype is capable of

importing a surplus of substrate. The rhamnose that were labelled uniformly with tritium may have lost signal as more and more of the initial protons become displaced during catabolism. This is in stark contrast to the *rhaU* deletion mutant, Rlt243, which showed near wild-type levels of transport while exhibiting similar growth rates as the *rhaT* truncation mutants *(Richardson et al*. 2008). Since RhaU affects the interconversion of L- and D- rhamnose, these results show that growth on rhamnose can be slowed down through two different means.

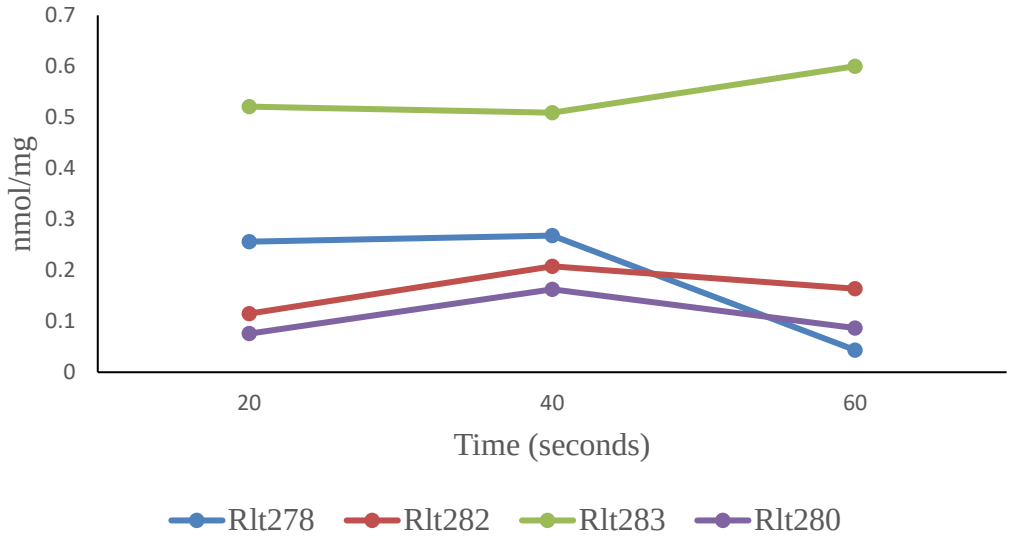

Figure 12. Uptake curve of *rhaT* truncation mutants.

The transport rate values are identical to Figure 8.

The main focus of this thesis was to investigate the relationship between CUT1 and CUT2 transporters. Prior to this study, the structure of a CUT1 ABC was thought to be monolithic. The alignment of CUT1 ABCs (Figure 6) revealed a major divide within the CUT1 family, primarily rooted in the presence of a 120 to 150AA C-terminal regulatory domain. This region was found to play a role in regulating the expression of its substrate-induced genes (Boos and Shuman, 1998). This regulatory region was stated to be a predominant feature of CUT1s (Schneider 2001). Meanwhile, four other CUT1 ABCs in that alignment showed no evidence of possessing such a region. On average, they were approximately 80-100 AA shorter in length than those of the MalK family. The overall layout of the core ABC motifs show clear differences between the structures (Figure 7). According to CDD, these ABCs belong to the MglA family. As stated previously, this family extends into CUT2 and includes RhaT. This raises the question of whether or not MglA ABCs are CUT1 or CUT2, and the relationship between its members that belong to different CUT types. The ones that are described as CUT1 fulfill all of the criteria for them to be deemed CUT1, and vice versa for CUT2. With these differences taken into account, this may suggest a common lineage between these transporters rather than MglA being exempt from the CUT classification. Combined with the ability to convert to CUT1 using truncation constructs, the relationship between MglA and MalK family of CUT1s show that the line between CUT1 and CUT2 is less certain than how it is described. There is another classification system (Types I, II, III) based on the mechanism of transport and structure of transmembrane domains (Locher 2016). In this system, it was revealed that the CUT2 ribose transporter in *E. coli* simultaneously exhibits traits attributed to Type I and Type II (Clifton *et al.* 2015). This shows that no current classification model is flawless.

One question that has yet to be resolved is where the interaction with RhaK fits in. The removal of the second NBD did not change the importance of RhaK as all of the truncation constructs showed RhaK-dependent growth on rhamnose. If anything, these constructs corroborate the previous finding in which RhaK exclusively interacts with the N-terminal fragment of RhaT (RhaTF1) (Rivers and Oresnik 2015). BLAST analysis shows that the Walker A / P-loop is situated in this region. As this region is responsible for ATP binding, the prevailing theory is that RhaK aids in binding or hydrolyzing ATP during the transport process. In CUT2 systems, there are no examples of this type of interaction aside from the rhamnose transporter in *Sinorhizobium meliloti* 1021. It is likely that the *S. meliloti* rhamnose transporter has a nearly identical mechanism of transport as it also requires a functional RhaK to transport. Like *R. leguminosarum*, the ability to catabolize and transport rhamnose also affects competition for nodule occupancy in *S. meliloti*.

The dependence on RhaK regardless of whether RhaT is a homogeneous dimer or a two-domain single peptide suggests that this trait is not specific to CUT2. This is corroborated by the recent findings in FrcA, another ABC protein in the MglA family, which possesses a similar structure to NBD1 in RhaT. FrcA initially became of interest due to possessing two kinases in the same operon. A work done by another member of our research group showed that disrupting one of these kinases adjacent to FrcA, annotated FrcK, was found to have a negligible effect on fructose phosphorylation. Furthermore, it was shown that the absence of FrcK resulted in a decrease in fructose uptake rate by half of the wild-type (Kohlmeier 2019). This is the second example of an ABC importer in the Rhizobiaceae which is affected by the presence of a kinase.

It is possible that both of these systems utilize the kinase through a similar mechanism. However, there is a fundamental difference in that the rhamnose importer requires RhaK for any uptake to occur whereas in the fructose transporter, it accounts for approximately 50%.

Since kinase-dependent transport have been observed in *R. leguminosarum* and *S. meliloti* so far, there is a possibility that this type of transport mechanism may be limited to a subset of rhizobia. As there is so much that have yet to be discovered for this interaction, it is difficult to ascertain the purpose of RhaK in transport or the underlying mechanism behind it. Despite a great deal of work being dedicated to the investigation of RhaK-RhaT, there is still much to explore. One subject of interest in the rhamnose transporter is the NBD2 P-loop. This motif has a substitution in its conserved lysine to arginine, which has been shown to prohibit ATP hydrolysis (Schneider and Hunke 1998). It is becoming more likely that RhaK affects ATP binding or hydrolysis in some regard. RhaK-dependent transport may be a consequence of the fact that RhaT only has ATP hydrolysis occurring in the region which interacts with RhaK. Since there is no evidence of RhaK interacting with RhaT in its NBD2, this domain is a potential candidate for enabling RhaK-independent ATP hydrolysis. Correcting this vestigial P-loop to a theoretically functional state may yield some mechanistic insight on how RhaK affects transport and how the numbers of active sites affect RhaK-dependent transport. It may also lead to interesting findings from the perspective of further progressing the CUT system. To directly tackle whether RhaK affects ATP hydrolysis or affects transport in a different way, an ATPase assay may also lead to some answers.

Regardless of the direction being taken, the development of a multigene complementation vector

will be instrumental in accelerating the characterization of the interaction. This will involve the construction of complementation vectors carrying a set of rhamnose transporter genes in tandem (*rhaSTPQ*, *rhaTPQ*, or *rhaRSTPQ*). Different combinations are necessary to resolve some uncertainties raised by the complementation experiment (Table 7). Although the substrate binding protein (RhaS) is an independent protein diffused throughout the periplasm, there is a possibility that it must also be included in the transcript (van der Heide and Poolman 2002). The inclusion of the negative regulator *rhaR* is to seek an explanation for the unexplainable patchy growth phenotype resulting from complementation with *rhaR*::Tn*5*. If a similar issue arises with complementation vectors without *rhaR*, its inclusion may be a strategy to resolve it.

Chapter 5:

Conclusions

This thesis aimed to explore the relationship between CUT1 and CUT2 transporters. Using *in silico* approaches, we designed and constructed two truncated variants of *rhaT* which forces the CUT2 rhamnose transporter to behave similarly to a CUT1 transporter. These new variants exhibited identical phenotypes as Rlt278, supporting the hypothesis that the truncated RhaT operates by forming a dimer of two copies. Between the two constructs we generated (Rlt282 and Rlt283), there were no significant differences in either growth rate or rhamnose accumulation, which suggests that the presence of the C-terminal tail in 285AA did not affect its performance (Table 5).

During the design process of CUT1-like RhaT, a divide within the CUT1 family was discovered. The two representative families studied, MglA and MalK, showed major differences in its motif layout (Figure 6). In addition to lacking a C-terminal regulatory domain and being around 80-100AA shorter, MglA family transporters appear to have more in common with the CUT2 RhaT than any CUT1 protein in the MalK family. Furthermore, RhaT was also annotated as a MglA family, suggesting that MglA family ABCs span across CUT1 and CUT2.

While this investigation began with the intent of complementing *rhaT*, this gene was unable to be complemented as an isolated gene (Table 3). In this work, we have discovered that *rhaT* can be complemented as long as it is transcribed together with the other rhamnose transporter constituents (Table 7). This finding will likely aid future complementation studies involving genes encoding the rhamnose ABC transporter.

Literature Cited

Abrahams, J.P., Leslie, A.G.W., Lutter, R., and Walker, J.E. 1994. Structure at 2.8 Â resolution of F1-ATPase from bovine heart mitochondria. Nature **370**(6491): 621–628. doi:10.1038/370621a0.

Altschul, S.F., Gish, W., Miller, W., Myers, E.W., and Lipman, D.J. 1990. Basic local alignment search tool. J. Mol. Biol. **215**(3): 403–410. doi:10.1016/S0022-2836(05)80360-2.

Ames, G.F.L. 1986. Bacterial periplasmic transport systems: structure, mechanism, and evolution. Annu. Rev. Biochem. **55**(1): 397–425. doi:10.1146/annurev.bi.55.070186.002145.

Badia, J., Baldoma, L., Aguilar, J., and Boronat, A. 1989. Identification of the *rhaA*, *rhaB* and *rhaD* gene products from *Escherichia coli* K-12. FEMS Microbiol. Lett. **65**: 253–258.

Baldani, J.I., Weaver, R.W., Hynes, M.F., and Eardly, B.D. 1992. Utilization of carbon substrates, electrophoretic enzyme patterns, and symbiotic performance of plasmid-cured clover rhizobia. Appl. Environ. Microbiol. **58**(7): 2308–2314.

Barona, A., Etxebarria, B., Aleksanyan, A., Gallastegui, G., Rojo, N., and Diaz-Tena, E. 2018. A unique historical case to understand the present sustainable development. Sci. Eng. Ethics **24**(1): 261–274. doi:10.1007/s11948-017-9891-5.

Beringer, J.E. 1974. R Factor Transfer in *Rhizobium leguminosarum*. J. Gen. Microbiol. (84): 188–198.

Biemans-Oldehinkel, E., Doeven, M.K., and Poolman, B. 2006. ABC transporter architecture

and regulatory roles of accessory domains. FEBS Lett. **580**(4): 1023–1035. doi:10.1016/j.febslet.2005.11.079.

Bisseling, T. 2002. Nod factor perception and signalling. Plant Soil: 239–249. doi:10.1105/tpc.002451.These.

Blüschke, B., Eckey, V., Kunert, B., Berendt, S., Landmesser, H., Portwich, M., Volkmer, R., and Schneider, E. 2007. Mapping putative contact sites between subunits in a bacterial ATP-binding cassette (ABC) transporter by synthetic peptide libraries. J. Mol. Biol. **369**(2): 386–399. doi:10.1016/j.jmb.2007.03.043.

Borths, E.L., Poolman, B., Hvorup, R.N., Locher, K.P., and Rees, D.C. 2005. In vitro functional characterization of BtuCD-F, the *Escherichia coli* ABC transporter for vitamin B_{12} uptake. Biochemistry **44**(49): 16301–16309. doi:10.1021/bi0513103.

Clifton, M.C., Simon, M.J., Erramilli, S.K., Zhang, H., Zaitseva, J., Hermodson, M.A., and Stauffacher, C. V. 2015. *in vitro* reassembly of the ribose ATP-binding cassette transporter reveals a distinct set of transport complexes. J. Biol. Chem. **290**(9): 5555–5565. doi:10.1074/jbc.M114.621573.

Corradi, N., and Bonfante, P. 2012. The arbuscular mycorrhizal symbiosis: origin and evolution of a beneficial plant infection. PLoS Pathog. **8**(4): e1002600. doi:10.1371/journal.ppat.1002600.

Daus, M.L., Berendt, S., Wuttge, S., and Schneider, E. 2007. Maltose binding protein (MalE) interacts with periplasmic loops P2 and P1 respectively of the MalFG subunits of the maltose ATP binding cassette transporter (MalFGK2) from *Escherichia coli*/*Salmonella*

during the transport cycle. Mol. Microbiol. **66**(5): 1107–1122. doi:10.1111/j.1365-2958.2007.05982.x.

Davidson, A.L., Dassa, E., Orelle, C., and Chen, J. 2008. Structure, function, and evolution of bacterial ATP-binding cassette systems. Microbiol. Mol. Bio. Rev. **72**(2): 317–364, table of contents. doi:10.1128/MMBR.00031-07.

Davidson, A.L., Shuman, H.A., and Nikaido, H. 1992. Mechanism of maltose transport in *Escherichia coli*: transmembrane signaling by periplasmic binding proteins. Proc. Natl. Acad. Sci. U. S. A. **89**(6): 2360–2364. doi:10.1073/pnas.89.6.2360.

Delgado-Baquerizo, M., Oliverio, A.M., Brewer, T.E., Benavent-González, A., Eldridge, D.J., Bardgett, R.D., Maestre, F.T., Singh, B.K., and Fierer, N. 2018. A global atlas of the dominant bacteria found in soil. Science (80-.). **359**(6373): 320–325. doi:10.1126/science.aap9516.

Ding, H., Yip, C.B., Geddes, B.A., Oresnik, I.J., and Hynes, M.F. 2012. Glycerol utilization by *Rhizobium leguminosarum* requires an ABC transporter and affects competition for nodulation. Microbiology **158**(5): 1369–1378. doi:10.1099/mic.0.057281-0.

Dowling, D.N., and Broughton, W.J. 1986. Competition for nodulation of legumes. Annu. Rev. Microbiol. **40**(1): 131–157. doi:10.1146/annurev.mi.40.100186.001023.

Downie, J.A., and Walker, S.A. 1999. Plant responses to nodulation factors. Curr. Opin. Plant Biol. **2**(6): 483–489. doi:10.1016/S1369-5266(99)00018-7.

Ehrhardt, D.W., Wais, R., and Long, S.R. 1996. Calcium spiking in plant root hairs responding to *Rhizobium* modulation signals. Cell **85**(5): 673–681. doi:10.1016/S0092-8674(00)81234-

9.

Eitinger, T., Rodionov, D.A., Grote, M., and Schneider, E. 2011. Canonical and ECF-type ATP-binding cassette importers in prokaryotes: Diversity in modular organization and cellular functions. FEMS Microbiol. Rev. **35**(1): 3–67. doi:10.1111/j.1574-6976.2010.00230.x.

Erisman, J.W., Galloway, J.N., Dise, N.B., Sutton, M.A., Bleeker, A., Grizzetti, B., Leach, A.M., and Vries, W. De. 2015. Nitrogen: too much of a vital resource. Sci. Br. (April): 1–48. doi:10.13140/RG.2.1.3664.8163.

Ernst, R., Kueppers, P., Klein, C.M., Schwarzmueller, T., Kuchler, K., and Schmitt, L. 2008. A mutation of the H-loop selectively affects rhodamine transport by the yeast multidrug ABC transporter Pdr5. Proc. Natl. Acad. Sci. U. S. A. **105**(13): 5069–5074. doi:10.1073/pnas.0800191105.

Esseling, J.J., Lhuissier, F.G.P., and Emons, A.M.C. 2003. Nod factor-induced root hair curling: continuous polar growth towards the point of nod factor application. Plant Physiol. **132**(4): 1982-1988. doi: 10.1104/pp.103.021634.

Finan, T.M., Hirsch, A.M., Leigh, J.A., Johansen, E., Kuldau, G.A., Deegan, S., Walker, G.C., and Signer, E.R. 1985. Symbiotic mutants of *Rhizobium meliloti* that uncouple plant from bacterial differentiation. Cell **40**(4): 869–877. doi:10.1016/0092-8674(85)90346-0.

Finan, T.M., Kunkel, B., De Vos, G.F., and Signer, E.R. 1986. Second symbiotic megaplasmid in *Rhizobium meliloti* carrying exopolysaccharide and thiamine synthesis genes. J. Bacteriol. **167**(1): 66–72. doi:0021-9193/86/070066-05$02.00/0.

Geddes, B.A., and Oresnik, I.J. 2014. Physiology, genetics, and biochemistry of carbon

metabolism in the alphaproteobacterium *Sinorhizobium meliloti*. Can. J. Microbiol. **60**(May): 491–507. doi:10.1139/cjm-2014-0306.

Giraud, M.F., and Naismith, J.H. 2000. The rhamnose pathway. Curr. Opin. Struct. Biol. **10**(6): 687–696. doi:10.1016/S0959-440X(00)00145-7.

Gould, A.D., and Shilton, B.H. 2010. Studies of the maltose transport system reveal a mechanism for coupling ATP hydrolysis to substrate translocation without direct recognition of substrate. J. Biol. Chem. **285**(15): 11290–11296. doi:10.1074/jbc.M109.089078.

Grote, M., Bordignon, E., Polyhach, Y., Jeschke, G., Steinhoff, H.J., and Schneider, E. 2008. A comparative electron paramagnetic resonance study of the nucleotide-binding domains' catalytic cycle in the assembled maltose ATP-binding cassette importer. Biophys. J. **95**(6): 2924–2938. doi:10.1529/biophysj.108.132456.

Hanahan, D. 1983. Studies on transformation of *Escherichia coli* with plasmids. J. Mol. Biol. **166**(4): 557–580. doi:10.1016/S0022-2836(83)80284-8.

van der Heide, T., and Poolman, B. 2002. ABC transporters: One, two or four extracytoplasmic substrate-binding sites? EMBO Rep. **3**(10): 938–943. doi:10.1093/embo-reports/kvf201.

Hopfner, K.P. 2016. Invited review: Architectures and mechanisms of ATP binding cassette proteins. Biopolymers **105**(8): 492–504. doi:10.1002/bip.22843.

Huang, J.-M., Baker, B.J., Li, J.-T., and Wang, Y. 2019. New microbial lineages capable of carbon fixation and nutrient cycling in deep-sea sediments of the Northern South China Sea. Appl. Environ. Microbiol. **85**(15). doi:10.1128/aem.00523-19.

Hvorup, R.N., Goetz, B.A., Niederer, M., Hollenstein, K., Perozo, E., and Locher, K.P. 2007. Asymmetry in the structure of the ABC transporter - binding protein complex BtuCD-BtuF. Science **317**(5843): 1387–1390. doi:10.1126/science.1145950.

Hyde, S.C., Emsley, P., Hartshorn, M.J., Mimmack, M.M., Gileadi, U., Pearce, S.R., Gallagher, M.P., Gill, D.R., Hubbard, R.E., and Higgins, C.F. 1990. Structural model of ATP-binding proteing associated with cystic fibrosis, multidrug resistance and bacterial transport. Nature **346**(6282): 362–365. doi:10.1038/346362a0.

Jones, J.D.G., and Gutterson, N. 1987. An efficient mobilizable cosmid vector, pRK7813, and its use in a rapid method for marker exchange in *Pseudomonas fluorescens* strain HV37a. Gene **61**(3): 299–306. doi:10.1016/0378-1119(87)90193-4.

Jones, K.M., Kobayashi, H., Davies, B.W., Taga, M.E., and Walker, G.C. 2007. How rhizobial symbionts invade plants: the Sinorhizobium-Medicago model. Nat. Rev. Microbiol. **5**(8): 619–33. doi:10.1038/nrmicro1705.

Joseph, B., Korkhov, V.M., Yulikov, M., Jeschke, G., and Bordignon, E. 2014. Conformational cycle of the vitamin B_{12} ABC importer in liposomes detected by double electron-electron resonance (DEER). J. Biol. Chem. **289**(6): 3176–3185. doi:10.1074/jbc.M113.512178.

Kanehisa, M., and Goto, S. 2000. KEGG: kyoto encyclopedia of genes and genomes. Nucleic Acids Res. **28**(1): 27–30. doi:10.1093/nar/28.1.27.

Kelley, L.A., Mezulis, S., Yates, C.M., Wass, M.N., and Sternberg, M.J.E. 2015. The Phyre2 web portal for protein modeling, prediction and analysis. Nat. Protoc. **10**(6): 845–858. Nature Publishing Group. doi:10.1038/nprot.2015.053.

King, B.J., Hunt, S., Weagle, G.E., Walsh, K.B., Pottier, R.H., Canvin, D.T., and Layzell, D.B. 1988. Regulation of O_2 concentration in soybean nodules observed by *in situ* spectroscopic measurement of leghemoglobin oxygenation. Plant Physiol. **87**(2): 296–299. doi:10.1104/pp.87.2.296.

Kondorosi, E., Mergaert, P., and Kereszt, A. 2013. A paradigm for endosymbiotic life: cell differentiation of *Rhizobium* bacteria provoked by host plant factors . Annu. Rev. Microbiol. **67**(1): 611–628. doi:10.1146/annurev-micro-092412-155630.

Korkhov, V.M., Mireku, S. a, Veprintsev, D.B., and Locher, K.P. 2014. Structure of AMP-PNP-bound BtuCD and mechanism of ATP-powered vitamin B_{12} transport by BtuCD-F. Nat. Struct. Mol. Biol. **21**(12): 1097–9. Nature Publishing Group. doi:10.1038/nsmb.2918.

Lewinson, O., Lee, A.T., Locher, K.P., and Rees, D.C. 2010. A distinct mechanism for the ABC transporter BtuCD-BtuF revealed by the dynamics of complex formation. Nat. Struct. Mol. Biol. **17**(3): 332–338. Nature Publishing Group. doi:10.1038/nsmb.1770.

Lewinson, O., and Livnat-Levanon, N. 2017. Mechanism of action of ABC Importers : conservation , divergence , and physiological adaptations. J. Mol. Biol. **429**(5): 606–619. The Authors. doi:10.1016/j.jmb.2017.01.010.

Liu, H. 2014. Ammonia synthesis catalyst 100 years: practice, enlightenment and challenge. Chinese J. Catal. **35**(10): 1619–1640. doi:10.1016/S1872-2067(14)60118-2.

Livnat-Levanon, N., Gilson, A.I., Ben-Tal, N., and Lewinson, O. 2016. The uncoupled ATPase activity of the ABC transporter $BtuC_2D_2$ leads to a hysteretic conformational change, conformational memory, and improved activity. Sci. Rep. **6**(February): 1–12. Nature

Publishing Group. doi:10.1038/srep21696.

Locher, K.P. 2016. Mechanistic diversity in ATP-binding cassette (ABC) transporters. Nat. Struct. Mol. Biol. **23**(6): 487–93. doi:10.1038/nsmb.3216.

Marchler-Bauer, A., Bo, Y., Han, L., He, J., Lanczycki, C.J., Lu, S., Chitsaz, F., Derbyshire, M.K., Geer, R.C., Gonzales, N.R., Gwadz, M., Hurwitz, D.I., Lu, F., Marchler, G.H., Song, J.S., Thanki, N., Wang, Z., Yamashita, R.A., Zhang, D., Zheng, C., Geer, L.Y., and Bryant, S.H. 2017. CDD/SPARCLE: Functional classification of proteins via subfamily domain architectures. Nucleic Acids Res. **45**(D1): D200–D203. doi:10.1093/nar/gkw1129.

Mauchline, T.H., Fowler, J.E., East, A.K., Sartor, A.L., Zaheer, R., Hosie, A.H.F., Poole, P.S., and Finan, T.M. 2006. Mapping the *Sinorhizobium meliloti* 1021 solute-binding protein-dependent transportome. Proc. Natl. Acad. Sci. **103**(47): 17933–17938. doi:10.1073/pnas.0606673103.

McNeil, M., Darvill, A., Fry, S., and Albersheim, P. 1984. Structure and function of the primary cell walls of plants. Annu Rev Biochem. doi:10.1146/annurev.bi.53.070184.003205.

Mergaert, P., Uchiumi, T., Alunni, B., Evanno, G., Cheron, A., Catrice, O., Mausset, A.E., Barloy-Hubler, F., Galibert, F., Kondorosi, A., and Kondorosi, E. 2006. Eukaryotic control on bacterial cell cycle and differentiation in the Rhizobium-legume symbiosis. Proc. Natl. Acad. Sci. U. S. A. **103**(13): 5230–5235. doi:10.1073/pnas.0600912103.

Mistou, M.Y., Sutcliffe, I.C., and Van Sorge, N.M. 2016. Bacterial glycobiology: Rhamnose-containing cell wall polysaccharides in Gram-positive bacteria. FEMS Microbiol. Rev. **40**(4): 464–479. doi:10.1093/femsre/fuw006.

Miwa, H., Sun, J., Oldroyd, G.E.D., and Downie, J.A. 2006. Analysis of Nod-factor-induced calcium signaling in root hairs of symbiotically defective mutants of *Lotus japonicus*. Mol. Plant-Microbe Interact. **19**(8): 914–923. doi:10.1094/MPMI-19-0914.

Mortensen, L., Dandanell, G., and Hammer, K. 1989. Purification and characterization of the *deoR* repressor of *Escherichia coli*. EMBO J. **8**(1): 325–331. doi:10.1002/j.1460-2075.1989.tb03380.x.

Oldham, M.L., Chen, S., and Chen, J. 2013. Structural basis for substrate specificity in the *Escherichia coli* maltose transport system. Proc. Natl. Acad. Sci. U. S. A. **110**(45): 18132–18137. doi:10.1073/pnas.1311407110.

Oldham, M.L., Davidson, A.L., and Chen, J. 2008. Structural insights into ABC transporter mechanism. Curr. Opin. Struct. Biol. **18**(6): 726–733. doi:10.1016/j.sbi.2008.09.007.

Oldham, M.L., Khare, D., Quiocho, F.A., Davidson, A.L., and Chen, J. 2007. Crystal structure of a catalytic intermediate of the maltose transporter. Nature **450**(7169): 515–521. doi:10.1038/nature06264.

Oldroyd, G.E.D. 2013. Speak, friend, and enter: signalling systems that promote beneficial symbiotic associations in plants. Nat. Rev. Microbiol. **11**(4): 252–63. Nature Publishing Group. doi:10.1038/nrmicro2990.

Orelle, C., Ayvaz, T., Everly, R.M., Klug, C.S., and Davidson, A.L. 2008. Both maltose-binding protein and ATP are required for nucleotide-binding domain closure in the intact maltose ABC transporter. Proc. Natl. Acad. Sci. U. S. A. **105**(35): 12837–12842. doi:10.1073/pnas.0803799105.

Oresnik, I.J., Pacarynuk, L.A., O'Brien, S.A.P., Yost, C.K., and Hynes, M.F. 1998. Plasmid-encoded catabolic genes in *Rhizobium leguminosarum bv. trifolii*: evidence for a plant-inducible rhamnose locus involved in competition for nodulation. Mol. Plant. Microbe. Interact. **11**(12): 1175–1185. doi:10.1094/MPMI.1998.11.12.1175.

Patel, E.H., Paul, L. V., Patrick, S., and Abratt, V.R. 2008. Rhamnose catabolism in *Bacteroides thetaiotaomicron* is controlled by the positive transcriptional regulator RhaR. Res. Microbiol. **159**(9–10): 678–684. Elsevier Masson SAS. doi:10.1016/j.resmic.2008.09.002.

Patzlaff, J.S., Van der Heide, T., and Poolman, B. 2003. The ATP/substrate stoichiometry of the ATP-binding cassette (ABC) transporter OpuA. J. Biol. Chem. **278**(32): 29546–29551. doi:10.1074/jbc.M304796200.

Pinweha, P., Pumirat, P., Cuccui, J., Jitprasutwit, N., Muangsombut, V., Srinon, V., Boonyuen, U., Thiennimitr, P., Vattanaviboon, P., Cia, F., Willcocks, S., Bancroft, G.J., Wren, B.W., and Korbsrisate, S. 2018. Inactivation of bpsl1039-1040 ATP-binding cassette transporter reduces intracellular survival in macrophages, biofilm formation and virulence in the murine model of *Burkholderia pseudomallei* infection. PLoS One **13**(5): 1–17. doi:10.1371/journal.pone.0196202.

Poole, P., Ramachandran, V., and Terpolilli, J. 2018. Rhizobia: from saprophytes to endosymbionts. Nat. Rev. Microbiol. **16**(5): 291–303. Nature Publishing Group. doi:10.1038/nrmicro.2017.171.

Quandt, J., and Hynes, M.F. 1993. Versatile suicide vectors which allow direct selection for gene replacement in Gram-negative bacteria. Gene **127**(1): 15–21. doi:10.1016/0378-1119(93)90611-6.

Quiocho, F.A., and Ledvina, P.S. 1996. Atomic structure and specificity of bacterial periplasmic receptors for active transport and chemotaxis: Variation of common themes. Mol. Microbiol. **20**(1): 17–25. doi:10.1111/j.1365-2958.1996.tb02484.x.

Ravindranathan, P., Pasham, D., and Goel, A. 2019. Oligomeric proanthocyanidins (OPCs) from grape seed extract suppress the activity of ABC transporters in overcoming chemoresistance in colorectal cancer cells. Carcinogenesis **40**(3): 412–421. doi:10.1093/carcin/bgy184.

Rees, D.C., Johnson, E., and Lewinson, O. 2009. ABC transporters: the power to change. Nat. Rev. Mol. Cell Biol. **10**(3): 218–227. doi:10.1038/nrm2646.

Richardson, J.S., Carpena, X., Switala, J., Perez-Luque, R., Donald, L.J., Loewen, P.C., and Oresnik, I.J. 2008. RhaU of *Rhizobium leguminosarum* is a rhamnose mutarotase. J. Bacteriol. **190**(8): 2903–2910. doi:10.1128/JB.01120-07.

Richardson, J.S., Hynes, M.F., and Oresnik, I.J. 2004. A genetic locus necessary for rhamnose uptake and catabolism in *Rhizobium leguminosarum* bv. *trifolii*. J Bacteriol **186**(24): 8433–8442. doi:10.1128/JB.186.24.8433.

Richardson, J.S., and Oresnik, I.J. 2007. L-rhamnose transport is sugar kinase (RhaK) dependent in *Rhizobium leguminosarum* bv. *trifolii*. J. Bacteriol. **189**(23): 8437–8446. doi:10.1128/JB.01032-07.

Rivers, D.M.R., and Oresnik, I.J. 2013. Carbohydrate kinase (RhaK)-Dependent ABC transport of rhamnose in *Rhizobium leguminosarum* demonstrates genetic separation of kinase and transport activities. J. Bacteriol. **195**(15): 3424–3432. doi:10.1128/JB.00289-13.

Rivers, D.M.R., and Oresnik, I.J. 2015. The sugar kinase that is necessary for the catabolism of

rhamnose in *Rhizobium leguminosarum* directly interacts with the ABC transporter necessary for rhamnose transport. J. Bacteriol. **197**(24): 3812–3821. doi:10.1128/JB.00510-15.

Robledo, M., Jimenez-Zurdo, J.I., Velazquez, E., Trujillo, M.E., Zurdo-Pineiro, J.L., Ramirez-Bahena, M.H., Ramos, B., Diaz-Minguez, J.M., Dazzo, F., Martinez-Molina, E., and Mateos, P.F. 2008. *Rhizobium* cellulase $CelC_2$ is essential for primary symbiotic infection of legume host roots. Proc. Natl. Acad. Sci. **105**(19): 7064–7069. doi:10.1073/pnas.0802547105.

Rodionova, I.A., Li, X., Thiel, V., Stolyar, S., Stanton, K., Fredrickson, J.K., Bryant, D.A., Osterman, A.L., Best, A.A., and Rodionov, D.A. 2013. Comparative genomics and functional analysis of rhamnose catabolic pathways and regulons in bacteria. Front. Microbiol. **4**(DEC): 1–14. doi:10.3389/fmicb.2013.00407.

Saier, M.H. 2000. Families of transmembrane sugar transport proteins. Mol. Microbiol. **35**(4): 699–710. doi:10.1046/j.1365-2958.2000.01759.x.

Saier, M.H., Reddy, V.S., Tsu, B. V., Ahmed, M.S., Li, C., and Moreno-Hagelsieb, G. 2016. The Transporter Classification Database (TCDB): recent advances. Nucleic Acids Res. **44**(D1): D372–D379. doi:10.1093/nar/gkv1103.

Sambrook, J., and Russell, D.W. 2001. Molecular cloning: a laboratory manual. *In* Cold Spring Harbor Laboratory Press, 3rd edition. Cold Spring Harbour, NY.

Santelia, D., Vincenzetti, V., Azzarello, E., Bovet, L., Fukao, Y., Düchtig, P., Mancuso, S., Martinoia, E., and Geisler, M. 2005. MDR-like ABC transporter AtPGP4 is involved in

auxin-mediated lateral root and root hair development. FEBS Lett. **579**(24): 5399–5406. doi:10.1016/j.febslet.2005.08.061.

Saurin, W., Köster, W., and Dassai, E. 1994. Bacterial binding protein-dependent permeases: characterization of distinctive signatures for functionally related integral cytoplasmic membrane proteins. Mol. Microbiol. **12**(6): 993–1004. doi:10.1111/j.1365-2958.1994.tb01087.x.

Savci, S. 2012. An agricultural pollutant: chemical fertilizer. Int. J. Environ. Sci. Dev. **3**(1): 73–80. doi:10.7763/ijesd.2012.v3.191.

Schmitt, L., Benabdelhak, H., Blight, M.A., Holland, I.B., and Stubbs, M.T. 2003. Crystal structure of the nucleotide-binding domain of the ABC-transporter haemolysin B: identification of a variable region within ABC helical domains. J. Mol. Biol. **330**(2): 333–342. doi:10.1016/S0022-2836(03)00592-8.

Schmitt, L., and Tampe, R. 2002. Structure and mechanism of ABC transporters. Curr. Opin. Struct. Biol. **12**(6): 754–760. doi:10.1016/S0959-440X(02)00399-8.

Schneider, E. 2001. ABC transporters catalyzing carbohydrate uptake. Res. Microbiol. **152**(3–4): 303–310. doi:10.1016/S0923-2508(01)01201-3.

Schneider, E., Eckey, V., Weidlich, D., Wiesemann, N., Vahedi-Faridi, A., Thaben, P., and Saenger, W. 2012. Receptor-transporter interactions of canonical ATP-binding cassette import systems in prokaryotes. Eur. J. Cell Biol. **91**(4): 311–317. Elsevier GmbH. doi:10.1016/j.ejcb.2011.02.008.

Schneider, E., and Hunke, S. 1998. ATP-binding-cassette (ABC) transport systems: functional

and structural aspects of the ATP-hydrolysing subunits/domains. FEMS Microbiol. Rev. **22**: 22 (1): 1–20. doi:10.1016/S0168-6445(98)00002-3.

Schwartz, N.B., Abram, D., and Feingold, D.S. 1974. L-Rhamnulose 1-phosphate aldolase of *Escherichia coli*. Role of metal in enzyme structure. Biochemistry **13**(8): 1726–1730. doi:10.1021/bi00705a026.

Schweizer, H., Boos, W., and Larson, T.J. 1985. Repressor for the sn-glycerol-3-phosphate regulon of *Escherichia coli* K-12: Cloning of the *glpR* gene and identification of its product. J. Bacteriol. **161**(2): 563–566.

Shitan, N., Bazin, I., Dan, K., Obata, K., Kigawa, K., Ueda, K., Sato, F., Forestier, C., and Yazaki, K. 2003. Involvement of CjMDR1, a plant multidrug-resistance-type ATP-binding cassette protein, in alkaloid transport in *Coptis japonica*. Proc. Natl. Acad. Sci. **100**(2): 751–756. doi:10.1073/pnas.0134257100.

Simossis, V.A., and Heringa, J. 2005. PRALINE: A multiple sequence alignment toolbox that integrates homology-extended and secondary structure information. Nucleic Acids Res. **33**(SUPPL. 2): 289–294. doi:10.1093/nar/gki390.

Smil, V. 2011. Nitrogen cycle and world food production. World Agric. (Smil): 9–13. doi:30006.

Story, R.M., and Steitz, T.A. 1992. Structure of the *recA* protein–ADP complex. Nature **355**(6358): 374–376. doi:10.1038/355374a0.

Sutcliffe, I.C., and Russell, R.R. 1995. Lipoproteins of Gram-positive bacteria. J. Bacteriol. **177**(5): 1123–1128. doi:10.1128/jb.177.5.1123-1128.1995.

Tal, N., Ovcharenko, E., and Lewinson, O. 2013. A single intact ATPase site of the ABC

transporter BtuCD drives 5% transport activity yet supports full *in vivo* vitamin B_{12} utilization. Proc. Natl. Acad. Sci. U. S. A. **110**(14): 5434–5439. doi:10.1073/pnas.1209644110.

Terasaka, K., Blakeslee, J.J., Titapiwatanakun, B., Peer, W.A., Bandyopadhyay, A., Makam, S.N., Lee, O.R., Richards, E.L., Murphy, A.S., Sato, F., and Yazaki, K. 2005. PGP4, an ATP binding cassette p-glycoprotein, catalyzes auxin transport in *Arabidopsis thaliana* roots. Plant Cell **17**(11): 2922–2939. doi:10.1105/tpc.105.035816.

Timmers, A.C., Auriac, M.C., and Truchet, G. 1999. Refined analysis of early symbiotic steps of the Rhizobium-Medicago interaction in relationship with microtubular cytoskeleton rearrangements. Development **126**(16): 3617–28. Available from http://www.ncbi.nlm.nih.gov/pubmed/10409507.

Triplett, E.W., and Sadowsky, M. 1992. Genetics of competition for nodulation of legumes. Annu. Rev. Microbiol. **46**: 399–428.

Via, V.D., Zanetti, M.E., and Blanco, F. 2016. How legumes recognize rhizobia. Plant Signal. Behav. **11**(2): 1–6. Taylor & Francis. doi:10.1080/15592324.2015.1120396.

Vigonsky, E., Ovcharenko, E., and Lewinson, O. 2013. Two molybdate/tungstate ABC transporters that interact very differently with their substrate binding proteins. Proc. Natl. Acad. Sci. U. S. A. **110**(14): 5440–5445. doi:10.1073/pnas.1213598110.

Vincent, J.M. 1970. A Manual for the practical study of root nodule bacteria. *In* Blackwell Scientific. Oxford.

Wagner, M., Shen, L., Albersmeier, A., van der Kolk, N., Kim, S., Cha, J., Bräsen, C.,

Kalinowski, J., Siebers, B., and Albers, S.V. 2018. Sulfolobus acidocaldarius transports pentoses via a carbohydrate uptake transporter 2 (CUT2)-type ABC transporter and metabolizes them through the aldolase-independent Weimberg pathway. Appl. Environ. Microbiol. **84**(3): 1–19. doi:10.1128/AEM.01273-17.

Walker, J.E., Saraste, M., Runswick, M.J., and Gay, N.J. 1982. Distantly related sequences in the α- and β-subunits of ATP synthase, myosin, kinases and other ATP-requiring enzymes and a common nucleotide binding fold. EMBO J. **1**(8): 945–951. doi:10.1002/j.1460-2075.1982.tb01276.x.

Watanabe, S., and Makino, K. 2009. Novel modified version of nonphosphorylated sugar metabolism - An alternative L-rhamnose pathway of *Sphingomonas* sp. FEBS J. **276**(6): 1554–1567. doi:10.1111/j.1742-4658.2009.06885.x.

Watanabe, S., Saimura, M., and Makino, K. 2008. Eukaryotic and bacterial gene clusters related to an alternative pathway of nonphosphorylated L-rhamnose metabolism. J. Biol. Chem. **283**(29): 20372–20382. doi:10.1074/jbc.M801065200.

Xu, W., Zhang, W., Zhang, T., Jiang, B., and Mu, W. 2016. L-rhamnose isomerase and its use for biotechnological production of rare sugars. Appl. Microbiol. Biotechnol. **100**(7): 2985–2992. doi:10.1007/s00253-016-7369-z.

Ye, J., Coulouris, G., Zaretskaya, I., Cutcutache, I., Rozen, S., and Madden, T.L. 2012. Primer-BLAST: a tool to design target-specific primers for polymerase chain reaction. BMC Bioinformatics **13**: 134. doi:10.1186/1471-2105-13-134.

Zaitseva, J., Jenewein, S., Jumpertz, T., Holland, I.B., and Schmitt, L. 2005. H662 is the linchpin

of ATP hydrolysis in the nucleotide-binding domain of the ABC transporter HlyB. EMBO J. **24**(11): 1901–1910. doi:10.1038/sj.emboj.7600657.

Zheng, W.H., Västermark, Å., Shlykov, M.A., Reddy, V., Sun, E.I., and Saier, M.H. 2013. Evolutionary relationships of ATP-binding cassette (ABC) uptake porters. BMC Microbiol. **13**(1). doi:10.1186/1471-2180-13-98.

Zhou, Y., Ojeda-May, P., and Pu, J. 2013. H-loop histidine catalyzes ATP hydrolysis in the *E. coli* ABC-transporter HlyB. Phys. Chem. Chem. Phys. **15**(38): 15811–15815. doi:10.1039/c3cp50965f.